J. Astrophys. (1983) 4, 75-107

Abundance Analysis of Selected Cepheids and the Galactic Distribution of Metallicity

Sunetra Giridhar *Indian Institute of Astrophysics, Bangalore 560034*

Received 1983 January 18; accepted 1983 April 28

Abstract. We have determined the atmospheric abundances of selected Cepheids in order to study the large-scale chemical inhomogeneities across the galactic disk. The classical Cepheids were selected as probes to study the variation of metallicity in the galactic disk, because of their high intrinsic luminosity, small age and the existence of period-luminosity and period-age relationships. High dispersion spectra of programme stars WZ Sgr, X Sgr, ζ Gem, T Mon and SV Mon were obtained using the 102-cm reflector of Kavalur Observatory. The atmospheric abundances were determined by theoretically synthesizing the selected portions of the stellar spectrum and comparing with the observed spectra. In order to compute the theoretical spectrum, the formal solution of the equation of radiative transfer was numerically evaluated with the simplifying assumptions of local thermodynamical equilibrium, plane-parallel geometry and hydrostatic equilibrium. These assumptions are reasonably good for the metallic lines of F-G supergiants and hence the observations were confined to the phases where Cepheids behave like nonvariable F-G supergiants.

The atmospheric abundances of iron-peak elements, Fe, Cr, Ti, Ca and heavier *s*-process elements Y, Ba, La, Ce, Sm were obtained by synthesizing a selected spectral region in the range 4330 Å – 4650 Å. We derive a radial abundance gradient for iron

$$\frac{d[\mathrm{Fe/H}]}{dr_{\mathrm{gc}}} = -0.056 \pm 0.08$$

for the region of galactic disk between 6.7 and 10.9 kpc from the galactic centre (assuming $r_{\mathrm{gc}} = 8.5$ kpc for the Sun). This value agrees with the one obtained from the general sample of Cepheids for which spectroscopic abundances are available, and also with the existing photometric determinations, but is shallower than the one derived by Luck (1982).

Abundances of the elements derived in the present investigation do

not show any significant correlation with atomic number. Also the abundance ratio of *s*-process elements does not show any correlation with Fe. This lack of correlation for disk population stars shows the inadequacy of simple models of galactic chemical evolution and favours the infall models. Alternately, the evolution of [*s*/Fe] may be determined by the ratio of intermediate-mass stars (which contribute *s*-process nuclei) to high-mass stars (which contribute Fe peak nuclei). Thus the different behaviour of halo and disk population may indicate a difference in the mass spectrum of star formation.

Key words: Cepheids, abundances – Galaxy, radial abundance gradient – spectrum synthesis

1. Introduction

The importance of the abundance study of different astronomical objects lies in the clue it gives to the chemical history of the Galaxy. Big-bang cosmology predicts the primordial gas to consist only of hydrogen, helium and traces of lithium. Heavier elements were synthesized in the interiors of the stars by thermonuclear reactions. Enrichment of the interstellar medium has resulted from the processed material ejected by massive stars in advanced stages of their evolution. Large- and small-scale chemical inhomogenities in the Galaxy have an important bearing on the problem of galactic evolution. The observed radial abundance gradient in the disk of our Galaxy as well as in other large galaxies, abundance anomalies across the spiral arms and the abundance ratios of the elements formed by primary and secondary processes of nucleosynthesis provide observational tests of the models of galactic evolution.

1.1 *The Radial Abundance Gradient*

The presence of an abundance gradient of O/H, N/H and N/S in external galaxies has been reported by a number of workers from the observations of H II regions (Searle 1971; Comte 1975; Benvenuti, D'Odorico & Peimbert 1973 *etc*). For our Galaxy, Peimbert, Torres-Peimbert & Rayo (1978) derived a radial abundance gradient for O/N, N/H, N^+/S^+ and He/H from photoelectric observations of five H II regions covering a galactocentric distance range from 8.4 to 18.9 kpc. Hawley (1977) observed a large number of H II regions and derived shallower abundance gradients in O/H and N/H than those derived by Peimbert, Torres-Peimbert & Rayo (1978), and no gradient in the abundance ratio He/H, S/H, Ne/H. Torres-Peimbert & Peimbert (1977), Peimbert (1979), and Peimbert & Serrano (1980) derived radial abundance gradients in the Galaxy for O/H and N/H from observations of planetary nebulae. A summary of different O/H and N/H gradients derived by different investigators is given by Pagel & Edmunds (1981).

From Geneva photometry of a large number of G and K dwarfs, Grenon (1972) derived an abundance gradient for Fe. Mayor (1976) studied kinematic and photometric properties of a large number of F dwarfs and G-K giants and derived two values of metallicity gradient $d[\mathrm{Fe/H}]/dr_{gc} = 0.04$ for all the objects with eccentricities of their galactic orbits in the range 0.05-0.4 and $d[\mathrm{Fe/H/}]dr_{gc} = 0.10$ for relatively younger ob-

jects with eccentricities of their galactic orbits in the range 0.05-0.15. Janes & McClure (1972) and Janes (1977, 1979) derived the variation of metallicity across the galactic disc by DDO photometry of a large number of G and K gaints and open clusters. The radial abundance gradient derived by Janes (1979) is $d[\mathrm{Fe/H}]/dr_{\mathrm{gc}} = 0.05$. Harris (1981) derived the radial metallicity gradient $d[A/\mathrm{H}]dr_{\mathrm{gc}} = 0.07$ from observations of a large number of classical Cepheids in the Washington photometric system.

Apart from photometric attempts to determine abundance gradients, accurate spectroscopically-determined abundances of supergiants and Cepheids have also been used (Luck & Bond 1980; Luck & Lambert 1981, hereafter LL) in determining the radial abundance gradient. Combining the results of earlier investigations, Luck (1982) derived a radial abundance gradient of – 0.13 for iron which is somewhat steeper than the other determinations. Though the relatively small range of 3 kpc in distance increases the uncertainity in the gradient estimated by Luck, such an analysis should ultimately yield more accurate results as the sample is enlarged to larger distances. Besides, such analyses are indispensable for the calibration of a photometric reddening-free abundance index.

1.2 *The Choice of Classical Cepheids*

In the present investigation, we have selected classical Cepheids as probes to study the variation of metallicity across the galactic disc. The classical Cepheids as a group have five properties which make them perhaps the most suitable class of stars for studying the abundance variation in the Galaxy.

(1) Cepheids, like the non-variable supergiants, are intrinsically luminous objects and they can hence be observed at a considerable range of distances.

(2) They comprise a homogeneous population, their masses, ages and luminosities are closely related to their periods, and the total range in age is much less than the age of the galactic disk.

(3) There exists a tight period-luminosity-colour relationship for classical Cepheids (Sandage & Tammann 1969), which enables one to determine their distances with sufficient accuracy. The intrinsic luminosity of non-variable supergiants (which have been used in the past to determine the radial abundance gradient) is inferred on the basis of their luminosity class and spectral type. The accuracy of these estimates is rather low and is only slightly improved by an application of model atmospheres.

(4) Cepheids, like F-G supergiants, have a temperature range in which their spectra show a large number of metallic lines. Also, the temperature is not so high as to make non-LTE effects important and at the same time not low enough for the convection to have any serious effect.

(5) The classical Cepheids with periods longer than ten days are quite young objects and hence their atmospheric abundances – at least for Fe peak nuclei – reflect the chemical composition of the interstellar medium out of which they are formed.

In Section 2, we describe the observational data used in the present study and the reduction techniques employed. The method of computation of the theoretical spectra, justification of underlying assumptions and descriptions of various lines suitable for abundance determination are given in Section 3. The agreement between the observed and computed spectra for each star and abundances derived for all the

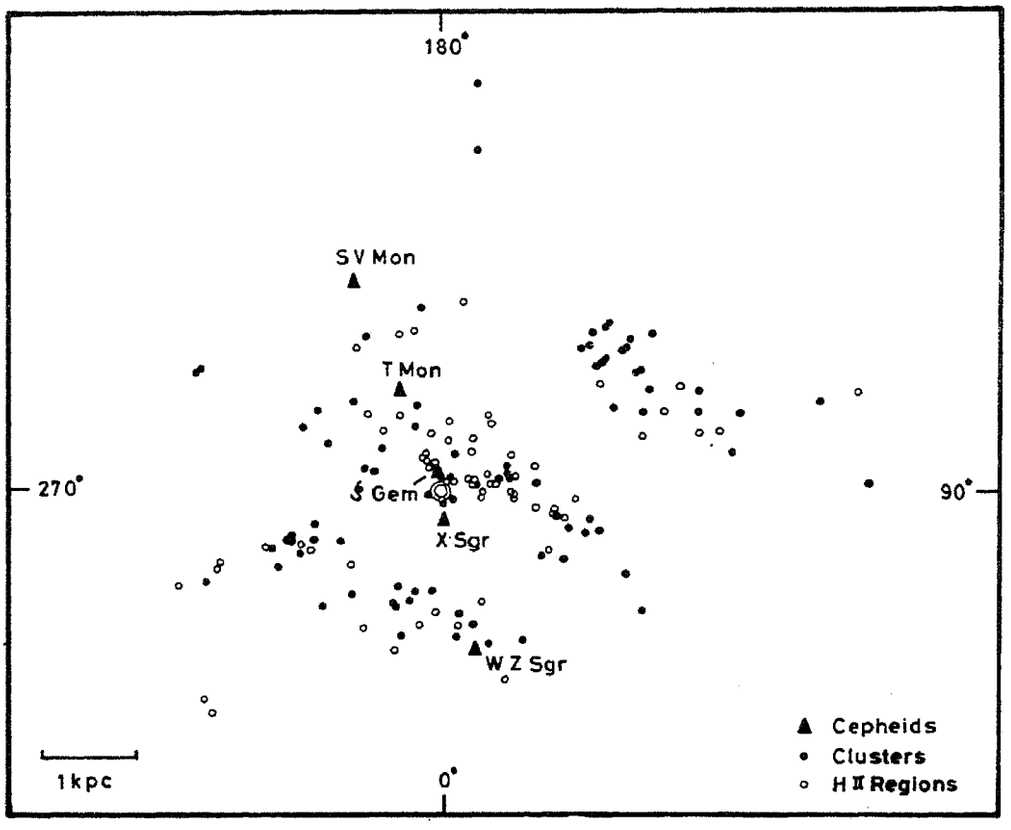

Figure 1. Distribution of programme Cepheids in the galactic plane. The optical spiral arms are defined using young open clusters and H II regions (Becker and Fenkart 1970.)

programme stars are presented in Section 4. The radial abundance gradient derived from the present work is compared with earlier estimates in Section 5. The good agreement between the gradient derived here and the earlier photometric estimates shows that there are no systematic errors in the photometry by previous investigators. In Section 6 we give an explanation of the results derived in the present study with an emphasis on the future prospects for an improvement of the techniques of analysis as well as for framing extensive observing programmes.

2. Observations

2.1 *Selection of Programme Stars*

The galactic distribution of all Cephids brighter than $m_v = 9.0$ was studied to select the stars suitable for abundance gradient determination. Fig. 1 shows the location of the programme stars in the galactic plane. The distribution of young open clusters and H II regions as determined by Becker & Fenkart (1970) are also shown in the same figure to bring out the spiral arms. We selected stars which lie approximately along a straight line from $l = 20°$ to $l = 100°$. The stars SV Mon and T Mon were chosen towards the galactic anticentre whereas X Sgr and WZ Sgr were chosen towards galactic

Table 1. Basic data on the programme stars.

Star	RA (1900) Dec (1900)	l deg b deg	Spectral type	V Max	V Min	P days	Epoch JD	r_{gc} kpc
X Sgr	17 41 16 −27 47.6	1.2 0.2	F5 – G1	4.24	4.84	7.0123	36968.85	8.13
ζ Gem	06 58 11 20 43.1	195.7 11.9	F7 – G3 Ib	3.66	4.16	10.1535	10639.80	8.87
T Mon	06 19 49 −07 08.4	203.6 −02.6	F7 – K1 Iab	5.59	6.60	27.0205	36137.09	10.14
SV Mon	06 16 04 06 30.9	203.7 −02.7	F8 – K5	7.8	8.9	15.2316	36437.07	10.87
WZ Sgr	18 11 06 −19 06.6	12.1 −01.4	G3 – K6	8.4	10.1	21.8497	35506.63	6.74

centre. ζ Gem is situated in the local arm. The sample of stars encompasses a range of 4.2 kpc around the Sun, − 2.5 kpc away from and 1.7 kpc towards the galactic centre. Table 1 contains the basic data on the programme stars. The coordinates, magnitudes, mean spectral types and luminosity classes are taken from Kukarkin *et al.* (1969). The distances listed in the table are calculated using the P-L-C relationship of Sandage & Tammann (1968) and using colour excesses of Nikolov & Ivanov (1974). The periods and the epochs of maxima are taken from Schaltenbrand & Tammann (1971).

2.2 *Details of Observational Data*

All the spectrograms used in the present investigation were obtained with the 102-cm reflector telescope of Kavalur Observatory. The Cassegrain spectrograph was used with a Varo 8605 single-stage image intensifier tube attached to it. The spectral region covered was 4300-4650Å.

ζ Gem and X Sgr were observed at a dispersion of 11.3 Å mm^{-1} using a 50-cm camera. The fainter stars, WZ Sgr and SV Mon were observed at a dispersion of 22.6Å mm^{-1} using a 25-cm camera. T Mon was observed at both these dispersions. The spectra were recorded on Kodak IIa-D or 103a-D plates. The projected slit width on the plates was 20μm. The spectra were widened between 0.3 - 0.5 mm depending upon the brightness of the star. Table 2 lists the details of observational data. The last two columns contain the duration of exposure as a fraction of pulsation period and the mean phase at the middle of exposure. Since all our programme stars have sufficiently long periods and the exposure times are always less than 150 min, it is reasonable to assume that there was no phase change during the exposure.

2.3 *Reduction Procedure*

The spectrograms were digitized using a Carl Zeiss microphotometer which has been automated using the microcomputer HCL Micro 2200 (Viswanath 1981). The digitized spectra were smoothed using three-point averages with weights 0.25, 0.50 and 0.25. Since the instrumental profile had a full width at half maximum (FWHM) of 35μm and the digitization interval was 8 μm, the 3-point triangular profile smoothens the spectra sufficiently without degrading the resolution. The smoothed spectra were

Table 2. Journal of observations.

Plate No.	Star	Dispersion Å mm^{-1}	Spectral region Å	Epoch of observation	Duration of exposure $\Delta\phi$	Phase ϕ
δ 1089	X Sgr	11.3	4300 – 4500	1980 Sep 26.604	0.0010	0.258
δ 1105	X Sgr	11.3	4400 – 4600	1980 Sep 27.595	0.0010	0.394
δ 1147	ζ Gem	11.3	4450 – 4650	1980 Oct 26.937	0.00015	0.238
δ 1180	ζ Gem	11.3	4450 – 4650	1980 Nov 7.915	0.00015	0.427
δ 1361	SV Mon	22.6	4300 – 4600	1981 Jan 31.737	0.0055	0.286
δ 1418	SV Mon	22.6	4300 – 4600	1981 Feb 16.625	0.0055	0.334
δ 1563	WZ Sgr	22.6	4200 – 4500	1981 Mar 24.958	0.0045	0.219
δ 1683	WZ Sgr	22.6	4400 – 4700	1981 Oct 9.708	0.0045	0.941
δ 1161	T Mon	11.3	4500 – 4700	1980 Nov 2.929	0.0012	0.219
δ 1182	T Mon	22.6	4300 – 4600	1980 Nov 30.845	0.0006	0.254

brought to the intensity scale using linear characteristic curves employing Baker densities (de Vaucouleurs 1968).

The effect of background exposures caused by undesirable light such as sky brightness or image-tube background is to reduce the S/N. The net S/N is related to the background exposure E_B and the total exposure $E_T = E_S + E_B$ by

$$(S/N)_{net} = \frac{(E_T - E_B)}{E_T} \; (S/N)$$

For our spectrograms, the density of the image-tube background was always between 0.02 and 0.04. It affected the S/N by only 5 to 10 per cent. After applying this correction, the S/N of our spectrograms was found to be ~ 120 and never below 100 even for the fainter stars. The application of a 3-point smoothing improved the S/N further by a factor of $\sqrt{2}$.

The observed spectrum is the convolution of the instrumental profile with the true flux spectrum. When a spectral line is intrinisically broadened (such as due to rotation in an early type star) rather than due to the instrumental profile, it is easy to deconvolve the observed spectrum from the instrumental profile and derive the true profile. However, when the stellar line width is comparable to the instrumental profile, the iterative method of deconvolution fails and the Fourier methods give rise to side lobes. It is more convenient to convolve the theoretical spectrum with the instrumental profile and then compare it with the observed spectrum.

We selected three weak unblended comparison lines of iron-argon hollow cathode lamp to determine the instrumental profile. The line centre x_0 was determined by parabolic interpolation. The shape of these profiles closely resembles a Gaussian profile. The parameters of the Gaussian profile were determined by using the linear relationship between log I and $(x - x_0)^2$. The FWHM of the apparatus profile corresponds to 0.40 Å at the dispersion of 11.3 Å mm^{-1} and 0.8 Å at the dispersion of 22.6 Å mm^{-1}. The observed spectrum is also broadened by stellar rotation (typically ~ 1 km s^{-1}) and macroturbulence (5-15 km s^{-1}). An inspection of the width of weak lines in our spectra showed that these effects were negligible with respect to the instrumental broadening.

3. Abundance analysis

Portions of stellar spectrum were synthesized using a suitable model for the atmosphere of the star and the atomic data of all the lines falling into the spectral region. The abundances of the contributing elements were adjusted till good agreement was obtained between the observed and computed spectra. For computation of the theoretical spectrum the formal solution of equation of radiative transfer was numerically evaluated for the line as well as the continuum flux. The spectrum synthesis programme of Sneden (1974) was used after slight modifications to reduce the memory requirement from ~ 100K to < 40K.

The theoretical spectrum was computed with the assumptions of (1) local thermodynamic equilibrium, (2) plane-parallel atmosphere and (3) hydrostatic equilibrium, which we proceed to justify in the following.

3.1 *Justification of Assumptions*

3.1.1 *Local thermodynamical equilibrium (LTE)*

The departure from LTE in low gravity stars has been discussed by Lites & Cowley (1974). These authors have investigated the formation of Fe I lines in stellar models of solar temperature, but in a range of surface gravities from Log $g = 2 - 4$. They have shown that it is only in the cores of strong lines that the departure from LTE becomes conspicuous. For the lines of moderate strength, the departure from LTE causes only a small difference in the equivalent widths and hence the assumption of LTE does not introduce significant errors in abundances if strong lines are excluded.

3.1.2 *Plane-parallel geometry*

When the extent of the atmosphere is much smaller than the radius of the star, we can consider plane-parallel geometry instead of concentric spheres. Low-gravity stars like giants and supergiants have extended atmospheres and the validity of this assumption

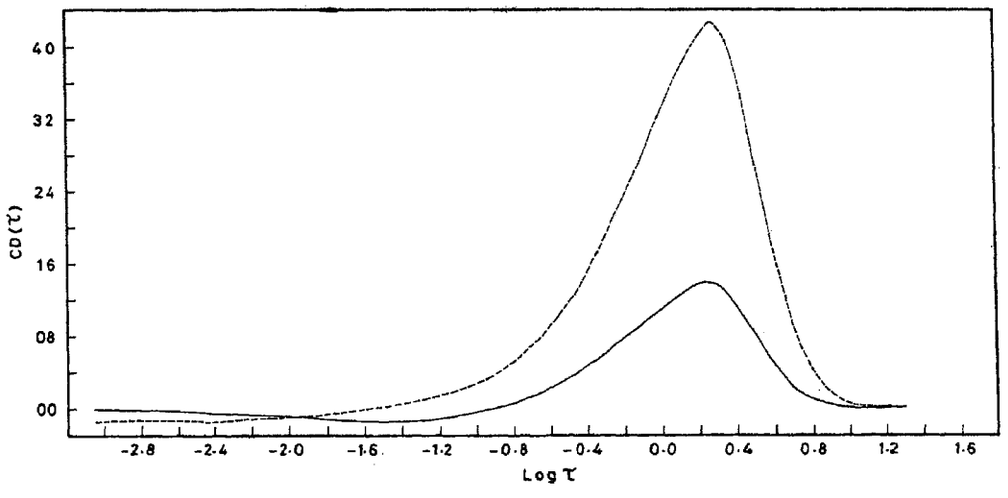

Figure 2. Contribution function of equivalent width is plotted as function of log τ for two lines (i) Fe I 4375.944 (E1 = 0.0 eV) shown by broken lines and (ii) Fe I 4625.052 (E1 = 3.2 eV) shown by continuous line.

could be questioned. But the assumption would still be valid if the extent of the line-forming region is much smaller than the radius of the star. In Fig. 2, we show the contribution function for the equivalent width as a function of optical depth for two lines of FeI with excitation potentials of 0.0 eV and 3.2 eV. We can see from the figure that the major contribution to the line comes from a narrow range in optical depth mainly between $\log \tau = 0.3$ to 0.8. The contribution function was calculated using a model with $T_e = 5500$ K and $\log g = 1.0$ from the grid of model atmospheres of Kurucz (1979). In these models, geometrical heights corresponding to different values of optical depths are also tabulated. FWHM of the contribution function corresponds to 84860 km in the geometrical height scale. If the radius of the star is assumed to be 60 $R_\odot$ which is a typical value for galactic Cepheids, the ratio of the line-forming region to the radius is 0.002. Furthermore, Gustafsson *et al.* (1975) have estimated the magnitude of the effect of dilution of radiation field due to sphericity and have obtained the corrections for the temperature scale. The temperature corrections for the sphericity, obtained by them are of the order of −70 K, −60 K, −50 K, and −30 K at $\log \tau = -4, -3, -2, -1$ respectively for models with $\log g = 0.75$. These corrections are very much smaller at higher gravities, particularly for the photospheric lines. Thus it is reiterated that the use of plane-parallel atomspheric layers will not introduce any serious errors in the computation of metallic lines.

3.1.3 *Hydrostatic equilibrium*

The assumption of hydrostatic equilibrium implies that there is no large-scale acceleration comparable to the surface gravity; hence the pressure balances the gravitational attraction. Such an assumption could be disrupted in the pulsating atmosphere of a Cepheid. Schmidt (1971) pointed out from his studies of a number of Cepheids that for long period Cepheids ($P > 10$ d) the spectroscopically derived surface gravities are in close agreement with those derived from their masses. Also, from the investigations of the density variations in a number of Cepheids (Rodgers & Bell 1968), Schmidt (1971) inferred that the hydrostatic equilibrium is maintained during most of the cycle for long-period Cepheids with small amplitudes. However for long-period Cepheids with large light variations, a sudden increase in density at the phase of strong outward acceleration was reported by Rodgers & Bell. Schmidt (1971) suggested that during the short interval of outward acceleration, gravity varies considerably, thereby affecting the hydrostatic equilibrium; however the atmosphere remains in hydrostatic equilibrium, for the rest of the cycle.

Keller & Mutschlecner (1970) calcuated a hydrodynamic model of a 11.5 d Cepheid. They also calculated hydrostatic constant-flux model atmospheres with parameters g_e and T_e taken from the hydrodynamic models at selected phases. The structures of these atmospheres compare well with hydrodynamic models; the $(B-V)$ colours predicted by the hydrostatic atmosphere and the hydrodynamic models show close agreement. These considerations also imply that properly chosen hydrostatic atmospheres can adequately predict the observable properties of Cepheids with $P > 10$ d.

Excepting X Sgr, all our programme stars have period > 10 d, and the light curve of X Sgr is very smooth without any suggestion of humps. All the stars were observed in a phase range where the acceleration of the atmosphere is minimum. Also, Kraft (1967) has pointed out that the resemblence of the Cepheid spectra with those of non-variable supergiants is closest at the phases corresponding to the falling branch of their

light curve. Pel (1978), while deriving the Intrinsic Cepheid Locus in the $(V-B)$ – $(B-L)$ diagram, found that the portions of these loops corresponding to the falling branch of the light curve are very similar for all the Cepheids and are least distorted. We feel that these phases are the most suitable ones for abundance determination as the assumption of hydrostatic equilibrium is best justified at these phases.

3.2 *Determination of the Atmospheric Parameters*

Pel (1978) determined the atmospheric parameters of a large number of Cepheids using Walraven five-colour photometry (Pel 1976). He derived temperatures, gravities, bolometric light curves, radius variation and equilibrium values of these quantities using the theoretical flux from Kurucz (1975) for a grid of model atmospheres covering a large range in temperature and gravity. He found that the $(V-B)$ – $(B-U)$ diagram is best suited for derivation of physical parameters, due to its sensitivity to temperature and gravity and also because it separates the two parameters well. He constructed a theoretical $(V-B)$ – $(B-U)$ diagram using the Kurucz models and fitted analytical expressions to the grid of theoretical colours and bolometric corrections.

In the region covered by the Cepheid loops, these relations fit the exact values of the discrete grid points within 0.0015 in θ_e and 0.05 in $\log g$. Pel computed this grid in the range $T_e = 5500-7000$ K and $\log g = 0.5 - 3.0$, and extrapolated the analytical relations down to $T_e = 5000$ K to cover the complete loops of Cepheids with $P > 11$ d. Though a majority of our programme stars have periods longer than this value, the phases on the descending branch of the light curve at which the observations were made have $T_e > 5400$ K and hence generally do not demand extrapolation. The initial estimates of T_e and $\log g$ were hence obtained using the analytical expressions of Pel (1978).

The photometrically-derived atmospheric parameters provide the first guess to the star's atmosphere. This guess is improved by computing a large number of lines covering a large range in equivalent widths, excitation potentials and at least two ionisation states for models with slightly differing atmospheric parameters. Different atmospheric parameters affect the strength of the lines in different ways, a fact that helps us in improving each atmospheric parameter independent of the others.

3.2.1 *Microturbulence*

Since it is known from the previous studies (*cf.* Schmidt 1971;LL) that the abundance of iron peak elements in Cepheids is not very different from the solar value, we have assumed the solar iron abundance as a starting value. We computed equivalent widths for a large number of lines covering a good range in equivalent widths using the model with T_e and $\log g$ determined photometrically and different trial values of microturbulent velocities. The microturbulent velocity was determined by requiring $W_{comp} - W_{obs}$ to be independent of the strength of the lines.

3.2.2 *Effective temperature*

In order to improve the estimate of effective temperature, lines of a particular element, say, iron are computed covering a large range in excitation potential. Abundances derived from individual lines are examined to see if they show a correlation with the excitation potential; such a correlation is expected if the effective temperature is incorrectly chosen. The elimination of such a correlation with excitation potential would lead to an improved choice of T_e.

3.2.3 *Surface gravity*

Once the temperature and microturbulent velocity are determined, the estimate of surface gravity can be improved by requiring that the lines of neutral and ionized iron lead to the same value of abundance.

3.3 *Assembling the Line Data*

The *s*-process elements present themselves in very few lines which are often blended. Very few attempts have been made in the past to determine the abundances of these elements and some of these determinations are even based on a single line. Obviously, such estimates are highly uncertain. Hence we have computed a number of small portions of the spectrum, each portion covering 5 Å to 15Å and having as many lines of Ba, La, Ce and Sm as possible.

The relevant atomic data of ~ 400 lines of interest is listed by Giridhar (1982). The wavelengths of the lines are taken from Moore, Minnaert & Houtgast (1966). The atomic mass and the ionisation potentials are taken from Allen (1973). The excitation potentials of upper and lower levels are taken from Moore (1945). The gf values were determined by an inverted solar analysis as described at the end of this section.

The spectral region 4550 Å–4564 Å proved to be extremely important in our investigations. Ba II 4554.036 is of great use because this line is relatively unblended for F and G spectral types in which most of the Cepheids fall. Shortward of this line, the first conspicuous line is Ti II 4552.29 which is not likely to affect the equivalent width or the central depth of the Ba II line. On the longer wavelength side, Cr II 4552.02 (multiplet 44) is present. The intensity of this line is not more than 50 per cent of the Ba II line. Fortunately, there are two more Cr II lines arising from the same multiplet in the same wavelength region (Cr II 4558.650 and Cr II 4588.204). These lines can be used to predict the behaviour of the Cr II 4555.02 line. Once an accurate value of chromium abundance is determined using other lines, the spectral region around 4554 Å can be computed with different barium abundances till a satisfactory agreement is reached. Also, an accurate gf value has been determined for Ba II 4554.036 by Holweger & Müller (1974).

However, Ba II 4554.036 is known to exhibit considerable hyperfine structure (Rutten 1976) with an effective width of 60 mÅ. Abt (1952) and Wolff & Wallerstein (1966) have shown that one could allow for this effect by using additional microturbulence for the affected line. Though the effect of hyperfine structure is not significant in supergiant atmospheres with their large turbulent velocities ($5 - 10\,\mathrm{km\,s^{-1}}$), it may be advisable to include it when highest precision is required.

Some investigators do not recommend the use of Ba II 4554.036 Å line because of its strength. This line does not fall on the linear portion of the curve of growth but on the flat portion where the lines are supposed to be more sensitive to microturbulence. However, an accurate value of microturbulence can be determined beforehand from the lines of elements like Fe, Cr, Ti *etc.* for which a large number of unblended lines of different intensities could be measured. Instead of being a disadvantage the strength of the line becomes an asset while working with low-dispersion spectra in which weak lines are almost lost due to the crowding of lines.

There are also important lines of Ce II at 4560.280 Å and 4562.367 Å. The resonance line 4562.367 Å is unblended. Its equivalent width is ~80 mÅ. Thus this line is on the linear portion of the curve of growth and hence well suited for abundance

determination. The lines that might interfere with these three lines are the following (i)Fe I 4560.097 Å is much weaker than Ce II 4560.280 for low-gravity atmospheres like Cepheids and hence not likely to affect the latter line. (ii) Fe I 4561.417 Å is even weaker than Fe I 4560.097 Å. It is found to be weak for all values of gravity. The solar equivalent width of this line is 1.3 m Å and it is not conspicuous in the photometric atlases of spectral lines of Procyon (F5 Ib) and Arcturus (K0). However, the atomic parameters of all these lines are included in the spectrum synthesis calculations. Since there is a large number of unblended Fe I and Fe II lines in the spectra, the abundance of Fe is determined very accurately and the effect of these contaminating lines could be eliminated. The resonance line 4562.367 Å is quite isolated and is one of the most suitable lines for abundance determination of Ce at the dispersion of 11.3 Å mm^{-1}.

At the lower dispersion of 22.6 Å mm^{-1}, which we employed for the fainter stars, Ce II 4560.280 Å and 4560.966 have merged together, but this blended feature can still be used for determining the abundance of Ce. Cowley (1970) has suggested the use of curve-of-growth technique even for blends. Blends are much easier to deal with in the method of spectrum synthesis. At the dispersion of 22.6 Å mm^{-1}, Ce II 4562.367 Å makes its presence felt as a hump in the wing of Ti II 4563.766. If the abundance of Ti is already determined using other lines, the hump at 4562.367 provides the information on the Ce abundance. The use of Ce II 4436.917 Å and 4628.160 Å is limited only to high dispersion spectra.

The important lines of samarium are Sm II 4329.038, 4334.166, 4362.038, 4420.526, 4577.694, and 4696.720. All these lines are useful at higher dispersions but Sm II 4334.166 and 4362.038 are the only ones that can be used at lower dispersions. The former line is blended with La II 4333.764 but the contribution of these lines could be separated. The line Sm II 4362.038 has no strong neighbouring lines to affect it. Ce II 4361.668 at its shorter wavelength side is extremely weak and Cr II 4362.93 at the longer wavelength side is also insignificant.

Among the line parameters required as input of the spectrum synthesis programme, accurate gf values for all the lines of interest are very difficult to get. The gf values have been experimentally derived by a number of workers using absorption or emission methods. These methods need accurate temperature measurements. To obtain an accuracy of 0.5 per cent in oscillator strengths, the temperature must be measured to an accuracy of 1.3 K at 3000 K which is extremely difficult to reach. The gf values determined by Blackwell & Shallis (1979) are by far the most accurate ones. They have determined these for a large number of Fe and Ti lines using the Oxford furnace technique. The accuracy of relative gf values determined by them is $\pm$ 0.5 per cent. However, very few of these lines fall in the spectral region of our interest. Wolnik & Berthel (1973), Foy (1972), Whaling, Scalo & Testerman (1977), May, Richler & Wichelmann (1974) and others have also experimentally determined gf values for a large number of lines but the accuracies of these estimates are not as high as those of Blackwell & Shallis. Also there are several weak lines for which experimental gf values have not been determined at all.

Kurucz & Peytremann (1975) have published a table of semi-empirical gf values which is the largest single list of identified spectral lines. These gf values have been determined semi-empirically using scaled Thomas-Fermi-Dirac radial wave functions and eigenvectors found through least-square fits to observed energy levels. They may not be as accurate as those of Blackwell & Shallis but still provide a huge amount of useful material. We used the gf values calculated by Kurucz & Peytremann as starting

values and improved them by inverted solar analysis. Solar abudances of various elements were taken from the new table of Pagel (1977). The solar photospheric model of Holweger & Müller (1974) was adopted with the depth independent microturbulent velocity of 1.0 km s^{-1}. The solar equivalent widths of Moore, Minnaert & Houtgast (1966) were used as input to the single-line version of the spectrum-synthesis programme. The *gf* values were altered by small amounts till the computed equivalent widths agreed with the observed ones. The values for the lines of iron-peak elements that have equivalent widths 50-250 mÅ did not require much alteration in inverted solar analysis. Strong lines, however, needed improvement. Also, for heavier elements like La, Ba, Ce, Sm the *gf* values derived by us differ from the input values for almost all the lines. Kurucz & Peytremann (1975) have pointed out that gf values of heavier elements could be improved when more atomic data are available.

Among the various intrinsic broadening, only Stark broadening affects the hydrogen lines. In the rarefied atmospheres of the supergiants, natural broadening predominates over collisional broadening. For the lines of weak and intermediate strength considered by us the total damping (natural + collisional) is very small, and may be neglected. We have, however included Van der Waals (collisonal) damping. The expression given by Unsöld (1955) was used, since it was readily available in Sneden's code, originally written for solar type dwarfs where this damping becomes important.

4. Abundance analyses of individual stars

We describe in this section the derivation of abundances for individual stars T Mon, ζGem, X Sgr, WZ Sgr and SV Mon. Three of our programme stars have been studied by LL using the spectrum synthesis method. These authors determined the abundances of C, N, O and a few heavier elements using high resolution reticon spectra in the red and near-infrared spectral regions. The resolution of these spectra obtained using a coudé reticon spectrometer is 0.2 Å which is better than the resolution (0.4 Å) of the present investigation. Also the red spectral region is much less crowded compared to the spectral region covered here. However, we cannot abandon the blue spectral region in favour of the red because the blue region contains many more important lines of heavy elements. In spite of the somewhat lower resolution of our spectrograms and entirely different spectral region of study, it is very satisfying to note the close agreement between the abundances derived by us and by LL. This success of the method of spectrum synthesis in dealing with the problems related to blending of the lines has lent support to our application of this method at still lower resolution.

4.1. *The Stars Observed at a Dispersion of 11.3 Å mm^{-1}*

T Monocerotis

T Monocerotis is a bright Cepheid with a pulsation period of 27.0205 d. Because of its brightness, it has been included in a number of investigations – photometric as well as spectroscopic. The light curve of this Cepheid is highly asymmetric but the variations in light are smooth with no suggestion of abrupt humps.

The atmospheric parameters of T Mon have been estimated by different workers at different phases of the star. These estimates are compared in Fig. 3. Our estimates of the atmospheric parameters are also plotted in the same figure. Schmidt (1972) determined the effective temperatures for a large number of Cepheids (including T Mon) by continuum photometry. He measured the slope of the Paschen continuum for

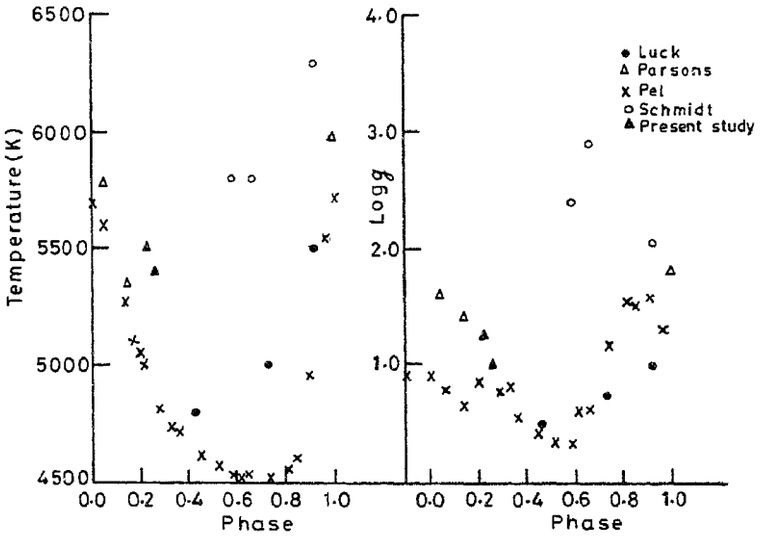

Figure 3. Atmospheric parameters of T Mon, as estimated by different investigators are plotted as a function of phase.

these stars and determined the temperature and line-blocking coefficients by a comparison with model-atmospheric energy distributions. The temperature derived by Schmidt are systematically hotter than ours by about 700 K. The temperatures derived by Pel (1978) using Walraven photometry are cooler by 250 K. Our temperatures are in fair agreement with the spectroscopically determined temperatures of LL and also with the temperatures derived by Parsons (1971) from the matching of observed *UVBGRI* colours with the model-atmospheric fluxes. Surface gravities derived by Pel and Parsons are in close agreement with the gravities derived in the present investigation ($\Delta \log g = \pm 0.5$) but the gravities derived by Schmidt, Rosendhal & Jewsbury (1974) are higher by $\Delta \log g = 1.6$. The probable reason is that the temperatures derived by Schmidt (1972) are too high and therefore to maintain ionisation balance, Schmidt, Rosendhal & Jewsbury were compelled to adopt higher gravities.

Table 3. Derived atmospheric parameters for the programme stars.

Star	Phase	T_{eff}	log g	ξ_T	12 + (log Fe/H)
X Sgr	0.258	6200	2.0	5.0	7.60
	0.394	6000	2.0	3.5	7.55
ζ Gem	0.238	5700	1.75	6.0	7.75
	0.427	5500	2.0	4.5	7.65
SV Mon	0.286	5800	1.5	5.0	7.40
	0.334	5600	1.5	5.0	7.40
WZ Sgr	0.219	5600	1.0	5.0	7.65
	0.941	6000	1.5	5.5	7.65
T Mon	0.219	5500	1.0	5.0	7.52
	0.255	5400	1.0	4.5	7.55

Table 4. Abundances of programme stars with respect to solar values.

Element	Z	Lines		T Mon	T Mon	X Sgr	X Sgr	WZ Sgr	WZ Sgr	SV Mon	SV Mon	ζ Gem	ζ Gem
		Max	Min	$\phi=0.219$	$\phi=0.255$	$\phi=0.258$	$\phi=0.394$	$\phi=0.941$	$\phi=0.219$	$\phi=0.286$	$\phi=0.334$	$\phi=0.238$	$\phi=0.427$
Ca	20	4	3	+0.10			−0.20					−0.10	−0.10
Sc	21	2	2		−0.20				+0.20	−0.15	−0.20	+0.10	+0.10
Ti	22	10	6	0.0	0.0	+0.15	+0.12	−0.20	+0.20	−0.15	−0.20	+0.10	+0.10
Cr	24	15	10	+0.05	+0.10	+0.20	+0.20	+0.25	+0.20	+0.10	+0.10	+0.30	+0.25
Fe	26	25	10	+0.02	+0.05	+0.10	+0.05	+0.15	+0.15	−0.10	−0.10	+0.25	+0.15
Y	39	1	1		−0.10						−0.10		
Ba	56	1	1	+0.10	+0.10		−0.02	+0.15		−0.10	−0.10	+0.05	+0.05
La	57	2	2		−0.10				+0.05	−0.20	−0.20		
Ce	58	5	2	+0.07	+0.07	−0.20	−0.20	−0.10		−0.30	−0.25	+0.15	+0.15
Sm	62	5	2	+0.02	−0.20	−0.20	−0.20		+0.10	−0.20	−0.20	+0.25	+0.20

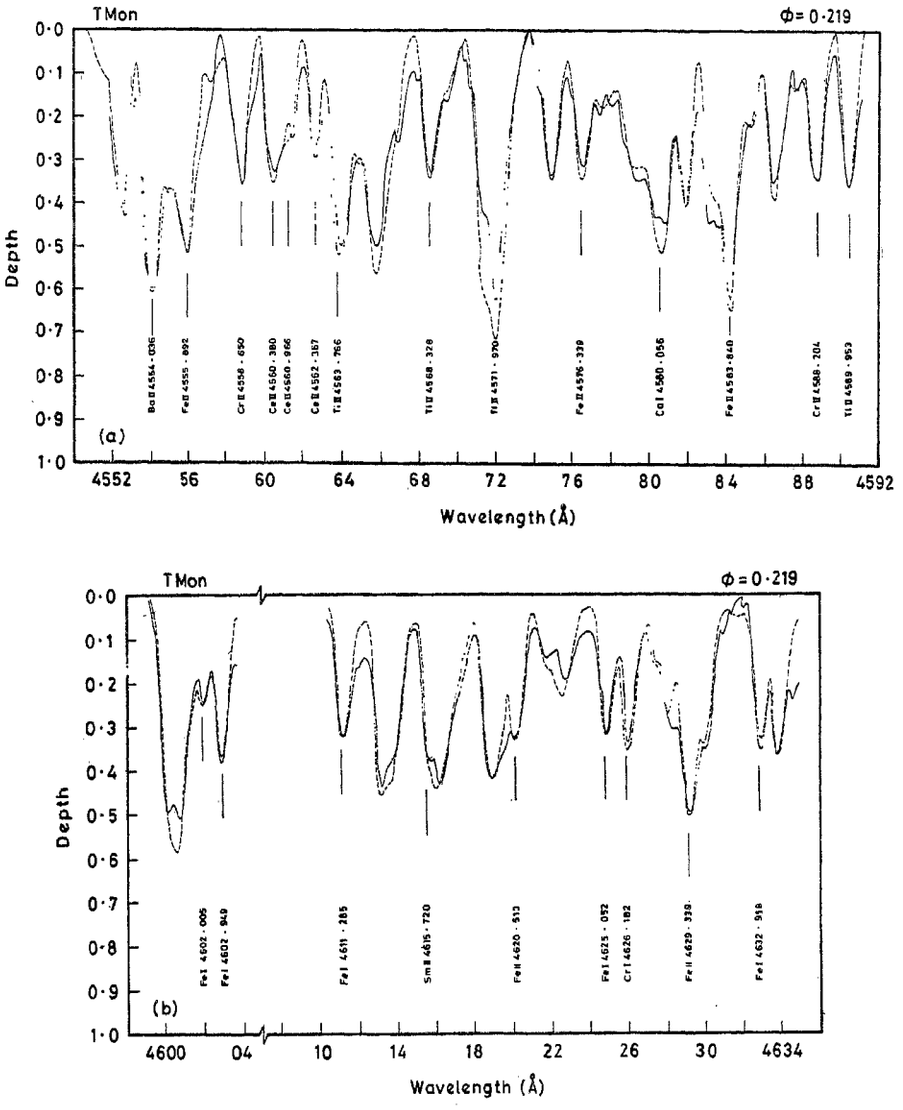

Figure 4. Observed (continuous line) and computed (broken line) spectra of T Mon.

Having determined the atmospheric parameters (Table 3), selected portions of the stellar spectrum were computed using models from the grid of Kurucz (1979) or Bell *et al.* (1976) with chemical abundances differing from the solar value by −0.3 to 0.3 dex in steps of 0.05 dex. Abundances of all the elements were varied by the same factor. The best fit abundances were thus determined. The agreement between the observed and computed spectra are shown in Fig. 4 which contains two sections of the spectrogram δ 1161 obtained at phase 0.219. The continuous line is the observed spectrum whereas the broken line is the computed one. The identifications and wavelengths of some of the important lines are also given in the figures. The final abundances for T Mon and the rest of the programme stars at observed phases are summarized in Table 4. The iron abundance computed by LL for T Mon is higher than our estimates by 0.09 dex; [Ce/Fe] computed by LL is also higher by the same amount.

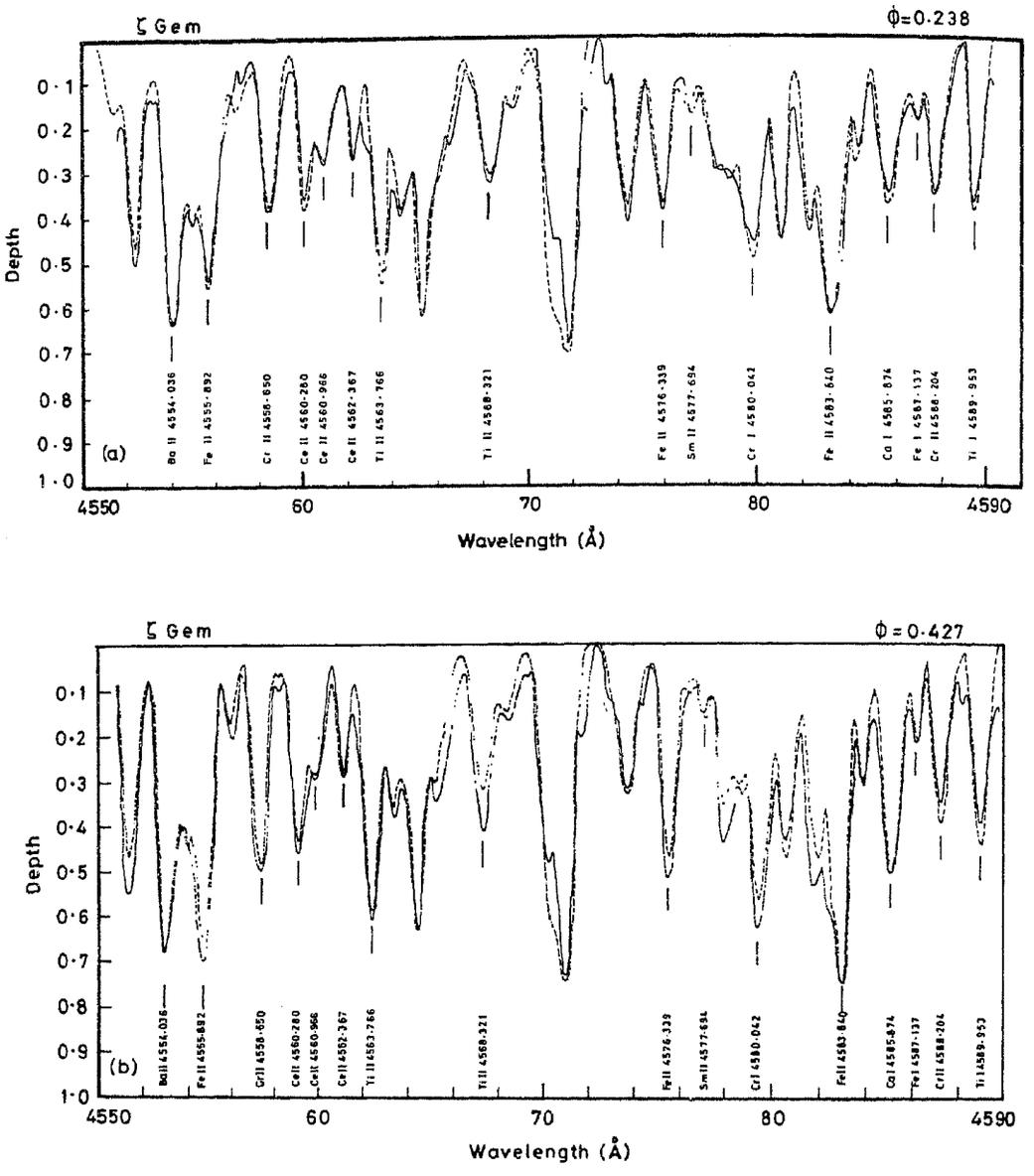

Figure 5. Observed (continuous line) and computed (broken line) spectra of ζ Gem.

4.1.2 *Zeta Geminorum*

The Cepheid ζ Gem is the prototype of Eggen's (1951) type C Cepheids with a nearly sinusoidal light curve and a period of 10.15 d. For this Cepheid, the temperatures are derived by Rautela & Joshi (1976) by matching the observed continuum energy distribution of the star with model-atmospheric fluxes of Parsons (1969). As compared to our spectroscopically derived temperatures, the temperatures estimated by Rautela & Joshi are systematically higher by 400 K. The temperatures determined by Parsons (1971) are cooler by 200 K, while the estimates of LL are in fair agreement with ours. The gravities derived by Rautela & Joshi, Parsons, and LL are all in fair agreement with our estimates ($\pm$0.5). Our observed and computed spectra of ζ Gem are shown in Fig 5. The iron abundance determined by LL is 0.13 dex higher than our

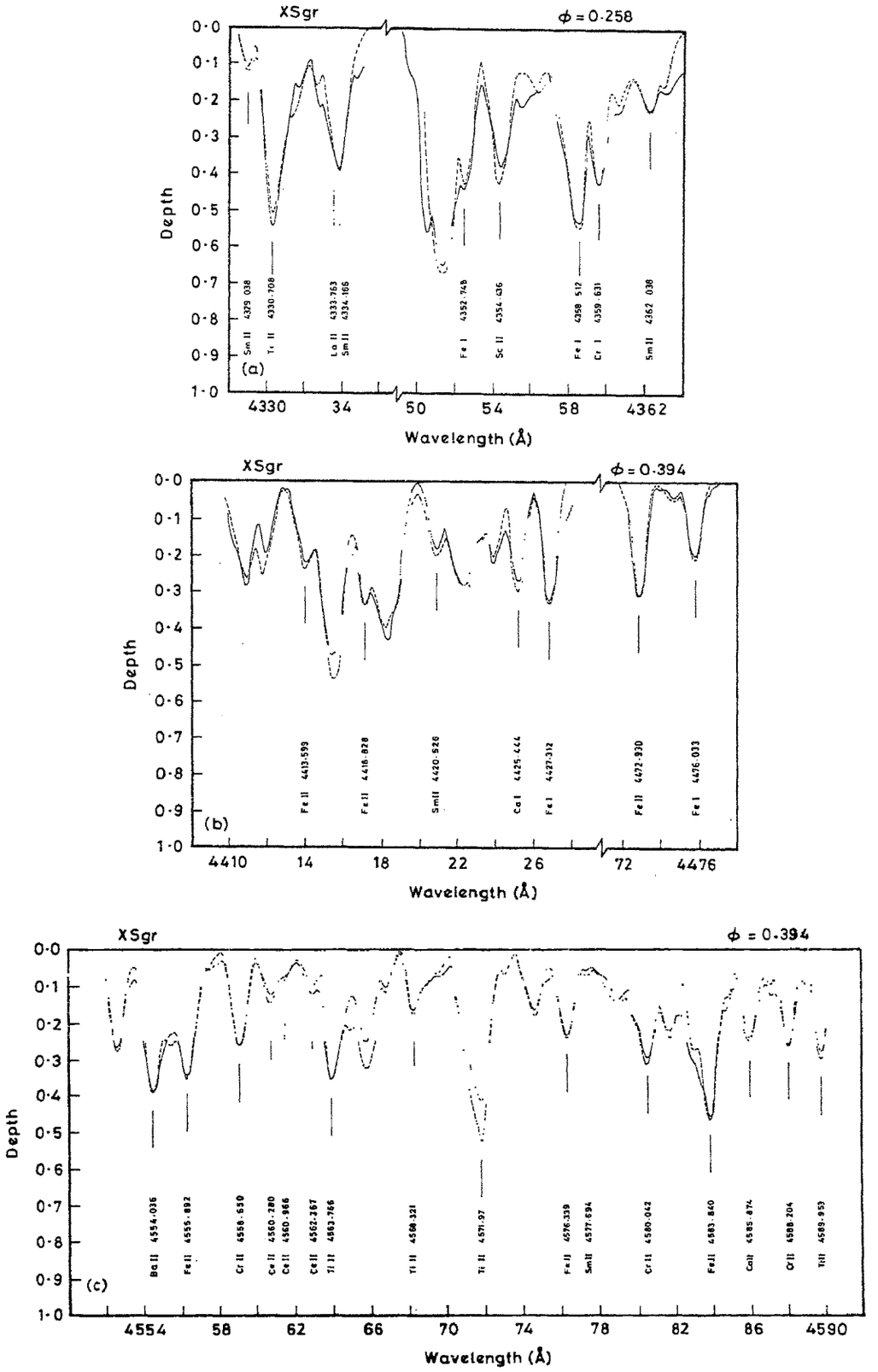

Figure 6. Observed (continuous line) and computed (broken line) spectra of X Sgr.

estimates while their estimate of [Ce/Fe] is lower by 0.07 dex.

4.1.3 X Sagittarii

UBV photometry of this bright southern Cepheid was done by Mitchell *et al.* (1964). Wisniewski & Johnson (1968) have determined the light curves in *UBVRIJKL* bands. Walraven, Tinbergen & Walraven (1964) and Pel (1976) have determined the light curves in *VBLUW* system. Light curves of X Sgr are asymmetric. Pel (1978) has reported some peculiarity in the two-colour loop in the $(B-L)-(V-B)$ diagram which is generally used to determine the colour excess. Evans (1968) examined the radial velocity curve derived by various investigators (*e.g.* Joy 1937; Stibbs 1955), but did not find any suggestion of a binary companion. High-resolution spectrophotometry in the ultraviolet (*e.g.* Mariska, Doschek & Feldman 1980) is more decisive in indicating the presence of faint photometric companions to Cepheids; an attempt needs to be made in this direction.

Despite being one of the brightest Cepheids in the southern sky, X Sgr has not been studied in great detail. Abundances of C, N, O and other heavier elements derived by LL are the first estimates of abundances so far. The iron abundance determined by LL is lower than ours by 0.05 dex. The agreement between the observed and computed spectra is shown in Fig. 6.

The mean abundances derived for the above three stars in this investigation are compared with the results of LL in Table 5.

4.2 *The Stars Observed at a Dispersion of 22.6 Å mm^{-1}*

The star T Monocerotis was observed at a dispersion of 11.3 Å mm^{-1} as well as 22.6 Å mm^{-1}. A comparison of the spectrograms obtained at the two dispersions helped us considerably in selecting the features which are useful even at the lower dispersion. The lines which are used for improving the estimates of the atmospheric parameters were selected based on the following criteria. The lines which are main contributors to a blend with no strong line in the close neighbourhood to affect their central depth were preferred. If a feature is made up of lines of the same element with no significant difference between the excitation potentials of the contributing lines, then the blend can be treated as a single line. Cowley (1970) has suggested the use of blend equivalent widths even in the curve-of-growth technique. Our investigation supports this idea. Ce II lines 4560.280 and 4560.966 which are seen well-resolved in Fig. 4

Table 5. Comparison of the abundances derived in this study with those of Luck & Lambert (1981). Abundances log (M/H) are given with respect to their solar value.

Element	X Sgr		ζ Gem		T Mon	
	LL	SG	LL	SG	LL	SG
Ti	−0.03	+0.13	+0.25	+0.10	+0.13	+0.00
Cr	+0.33	+0.20	+0.20	+0.27	+0.02	+0.07
Fe	+0.02	+0.07	+0.34	+0.20	+0.12	+0.03
Ba		−0.02		+0.05		+0.10
La	+0.32		+0.48		+0.50	−0.10
Ce		−0.20	+0.21	+0.15	+0.06	+0.07

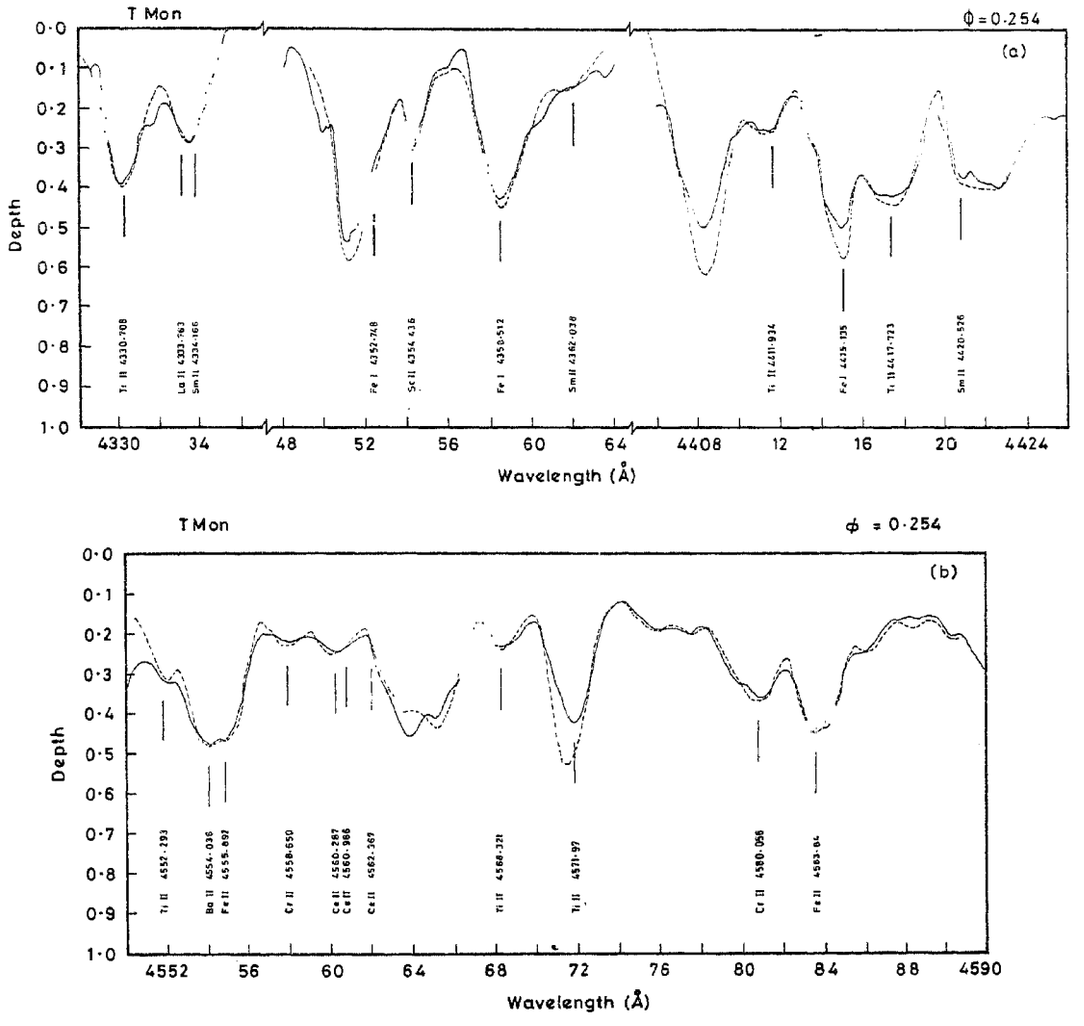

Figure 7. Observed (continuous line) and computed (broken line) spectra of T Mon at lower resolution.

present themselves as a single feature at the lower dispersion. The lower excitation potentials of these lines (0.43 eV and 0.20 eV) are not significantly different. This feature was found useful in determining the Ce abundance.

Abundances derived from the low-dispersion spectra of T Mon agree well with the ones derived using high-dispersion spectra. The observed and computed low-dispersion spectra shown in Fig. 7 demonstrate the utility of the method at lower dispersion.

4.2.1. *SV Monocerotis*

SV Mon is a relatively faint Cepheid ($m_v = 8.0$). The *UBV* light curves have been obtained by Mitchell *et al.* (1964) and Eggen (1969). *VBLUW* light curves have been obtained by Walraven, Tinbergen & Walraven (1964) and Pel (1976). Tsarevsky (1967) found some suggestion of variation in the period. The light curves are highly asymmetric. The radial velocity curve of SV Mon was derived by Joy (1937) using prismatic

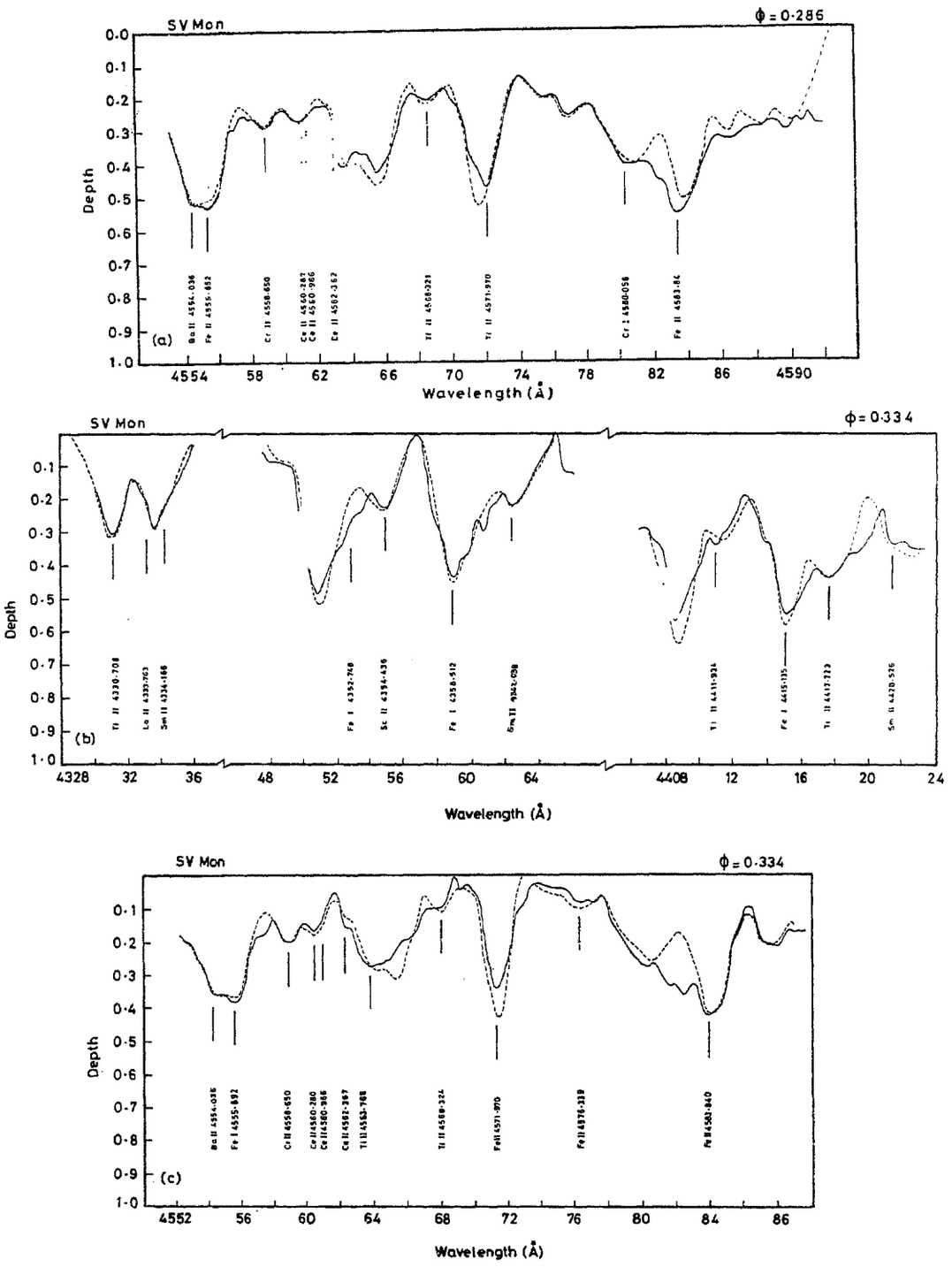

Figure 8. Observed (continuous line) and computed (broken line) spectra of SV Mon.

spectra. No further spectroscopic investigation is reported for this star so far. Spectroscopic abundances are derived for the first time in our investigations. Observed and computed spectra are shown in Fig. 8.

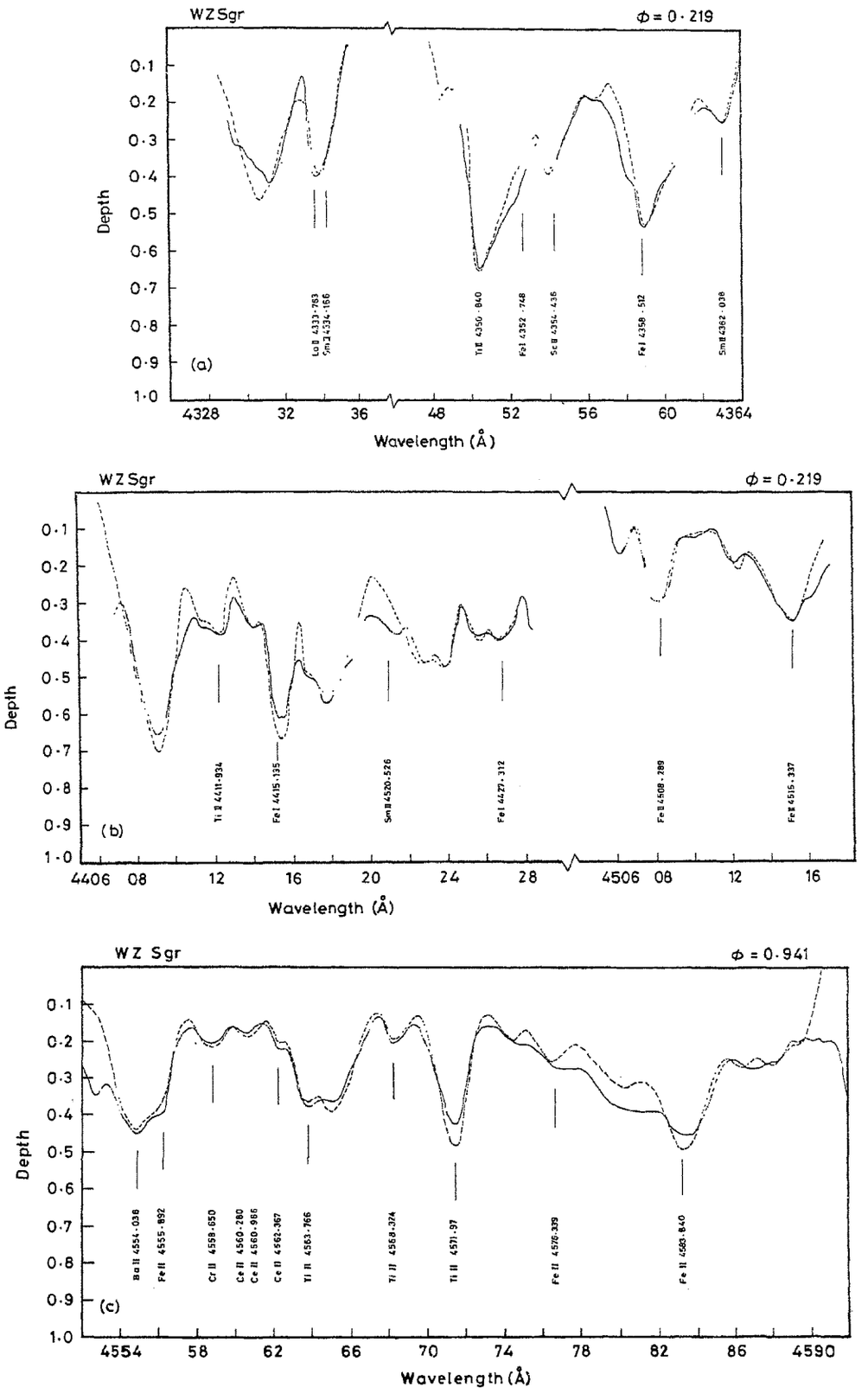

Figure 9. Observed (continuous line) and computed (broken line) spectra of WZ Sgr.

4.2.2. *WZ Sagittarii*

WZ Sgr is believed to be a member of Sgr-OB4 association (Tammann 1970). The light curves of this Cepheid in *UBV* have been determined by Mitchell *et al.* (1964) and in *VB-LUW* by Walraven, Tinbergen & Walraven (1964). Like SV Mon, spectroscopic abundances for WZ Sgr are determined for the first time in the present investigation. The agreement between the observed and computed spectra is shown in Fig. 9.

4.3 *Error Analysis*

There are two main sources of error in the abundances derived here:

(1) The errors in the input parameters like the observed equivalent width and the gf values manifest themselves as line-to-line scatter. The resultant error in aundances can be evaluated satisfactorily when the number of lines is large. For elements like Fe for which a large number of lines ($n > 20$) could be measured, typical standard deviation about the mean abundance is ~ 0.08 dex. For Cr and Ti fewer lines were measured ($n \sim 15$) and the standard deviation increases to $\pm$ 0.1 dex. For the elements with still fewer lines the errors are difficult to assess since the standard deviation loses its statistical meaning. The errors in such cases probably lie in the range of $\pm$ 0.20 – 0.25 dex.

(2) The uncertainties in the model atmospheric parameters would also introduce errors in abundances. For the estimation of these errors we computed a set of Fe lines for the pairs of the model atmospheres with (i) the same gravity and microturbulent velocity but different temperatures, (ii) the same temperature and gravity but different micro turbulent velocities, and (iii) the same temperature and microturbulent velocity but different gravities. A comparison of the variations in the computed equivalent widths for the three cases mentioned above, with the observational scatter, leads us to believe that the accuracy of the adopted effective temperature is $\pm$ 250K, that of $\log g$, $\pm$ 0.25 and that of microturbulent velocity, ± 0.5 km s^{-1}.

Errors in the abundances arising from the errors in atmospheric parameters are not the Gaussian sum of the errors due to the individual parameters. These parameters interact with one another. A change in one may cause a shift in another. The net effect on the derived abundances would be considerably less because we employ the principle of consistency wherein the lines with a large range of excitation potentials, equivalent widths and different inonization states should lead us to the same value of abundances. Therefore the errors in the derived abundances are not significantly larger than the errors estimated from the internal consistency check.

In the past, the abundances in Cepheid atmospheres were derived at different phases of their pulsation cycle and the average abundances were adopted. Amplitude of the variations in the derived abundances were quite large ($\pm$ 0.5 dex) in the investigations of Rodgers & Bell (1968 and references therein). The comparison of the abundances derived at different phases led LL to believe that the accuracy of the abundances derived by them was $\pm$ 0.2 dex. However, we feel that this practice of deriving the abundances at different phases and estimating the accuracy by the scatter around the mean values is not realistic. At the phases corresponding to the rising part of the light curve, *i.e.* from minimum light to maximum light, the atmosphere is moving very rapidly and hence the assumption of hydrostatic equilibrium is no longer valid. Thus the abundances derived at these phases are not very accurate. The accuracy can only be improved by making a large number of observations within the phase range 0.25 – 0.45 where the atmosphere of the star is neither expanding nor contracting and therefore the assumption of hydrostatic equilibrium is justified.

Table 6. Mean derived abundances with respect to the solar value.

Z	[X/Fe]	X Sgr	ζ Gem	SV Mon	WZ Sgr	T Mon	Mean
20	Ca/Fe	−0.27	−0.30			+0.08	−0.16
22	Ti/Fe	+0.06	−0.10	−0.07	−0.15	−0.03	−0.06
24	Cr/Fe	+0.13	+0.07	+0.20	+0.07	+0.05	+0.10
39	Y/Fe			0.0		−0.13	−0.06
56	Ba/Fe	−0.09	−0.15	0.0	0.0	+0.07	−0.03
57	La/Fe				−0.10	−0.10	−0.10
58	Ce/Fe	−0.27	−0.05	−0.17	−0.25	+0.04	−0.13
62	Sm/Fe	−0.27	+0.03	−0.10	−0.05	−0.12	−0.10

5. Results and conclusions

5.1 *Comparison with Earlier Investigations*

Elemental abundances have been reported in the literature for several Cepheids. The investigations of bright Cepheids by Rodgers & Bell (1968 and references therein) and Bappu & Raghavan (1969) showed marked underabundance of *s*-process elements in the Cepheid atmospheres. However, recent work of LL using the technique of spectrum synthesis does not confirm this trend. Although, relative to Fe, the *s*-process elements Ce and Nd are found to be underabundant compared to the solar values, the difference seldom exceeds 0.3 dex. La was found to be overabundant in some of the stars. Our investigation agrees with LL in that all the *s*-process elements are underabundant, the deficiency is of the same order and never exceeds 0.3 dex. The abundance ratio [X/Fe] defined by

$$[\mathrm{X/Fe}] = \log (\mathrm{X/Fe})_* - \log (\mathrm{X/Fe})_\odot$$

for various elements derived in the present study is given in Table 6. The individual elements fall into two groups: (i) the lighter elements with $20 \leq Z \leq 24$ and (ii) the heavier elements with $56 \leq Z \leq 62$ with yttrium ($Z = 39$) falling in between.

Within the errors of estimation, there are no systematic differences between [X/Fe] for different stars, except for a possible underabundance of Ti and Ca in WZ Sgr and ζ Gem. The [X/Fe] for lighter elements has a tendency to increase with Z and possibly a slight decreasing trend for heavier elements. Ca is deficient in all the stars and more conspicuously in X Sgr and ζ Gem. However, these differences are not significantly above the scatter in the individual abundances. Yttrium abundance was determined only for T Mon and SV Mon. The two values of [Y/Fe] have a mean of − 0.06. The heavier *s*-process elements show a general underabundance, the average value of [*s*/Fe] being − 0.09. Thus there is no evidence of *s*-processing or any other anomaly in the abundances of the sample stars.

5.2 *The Radial Gradient in* [Fe/H]

Fig. 10 shows the location in the galactic plane of Cepheids for which the spectroscopic abundances (listed in Table 7) are available. The outline of the spiral features are taken from Humphreys (1978) who used the associations of young stars, HII regions and young clusters to trace the optical features. The values of [Fe/H] for these stars are plotted as a function of their galactocentric distances (r_{gc}) in Fig. 11. A galactocentric distance of 8.5 kpc has been assumed for the sun in calculating these distances.

Different symbols have been used for different investigators. This enables us to see the systematic differences between various investigations, following the stars that have been included in two or three investigations. A straight-line fit to this data yields

$$[Fe/H] = -0.077\, r_{gc} + 0.707$$
$$\pm 0.035 \quad \pm 0.308$$

with a correlation coefficient of $r = -0.36$. The correlation is rather weak with a 10 per cent probability that it is purely due to random effects. Harris (1981), using the

Table 7. Compilation of spectroscopic abundances of Cepheids.

Star	r_{gc}	[Fe/H]	[Y/Fe]	[Ba/Fe]	[La/Fe]	[Ce/Fe]	[Sm/Fe]	Source
WZ Sgr	6.73	+0.15		0.00	−0.10	−0.25	−0.05	7
SV Vul	7.80	+0.28			+0.14	−0.04		6
S Nor	7.74	+0.10						3
Y Oph	7.86	+0.18						3
U Sgr	7.86	+0.10						3
W Sgr	8.03	+0.27.	+0.03		+0.30			6
χ Cyg	8.07	−0.42			−1.16	−1.25	−0.87	2
X Sgr	8.13	+0.02			+0.30			6
		+0.07		−0.09		−0.27	−0.27	7
η Aql	8.29	+0.06	−0.05		+0.45	+0.01		6
		+0.13						4
X Cyg	8.32	+0.15	+0.06		+0.16	+0.01		6
		+0.08		+0.23	+0.16	+0.13	+0.24	4
T Vul	8.33	−0.05	−0.19		−0.09			6
DT Cyg	8.41	+0.12	−0.05		+0.12			6
β Dor	8.49	+0.01	+0.28	+0.01	−0.28	−0.43	−0.64	2
δ Cep	8.57	+0.06	+0.06		+0.30	+0.08		6
		−0.06	+0.06	−0.04	−0.10	−0.06	−0.49	5
SU Cas	8.73	−0.12	+0.04		−0.03			6
ζ Gem	8.83	+0.34	−0.10		+0.14	−0.13		6
		+0.20		−0.15		−0.05	+0.03	7
RT Aur	8.96	−0.20	+0.16	−0.97	−0.98	−1.14	−0.56	1
		+0.06	−0.10		−0.10			6
TU Cas	9.02	−0.13	−0.08		+0.13			6
RS Pup	9.16	−0.07	+0.25			−0.09		6
T Mon	9.61	+0.12	+0.10		+0.38	−0.12		6
		+0.03		+0.07	−0.13	−0.03	−0.12	7
		+0.14		−0.03	−0.65	+0.05	+0.47	4
RX Aur	10.25	−0.37		−0.71	+0.44	+0.11	+0.54	4
SV Mon	10.87	−0.10		0.00	−0.10	−0.17	−0.10	7

Source:

1. Bappu & Raghavan (1969)
2. Rodgers & Bell (1968 and references therein)
3. Schmidt (1971)
4. Schmidt, Rosendhal & Jewsbury (1974)
5. Van Paradijs (1971)
6. Luck & Lambert (1981)
7. Present study

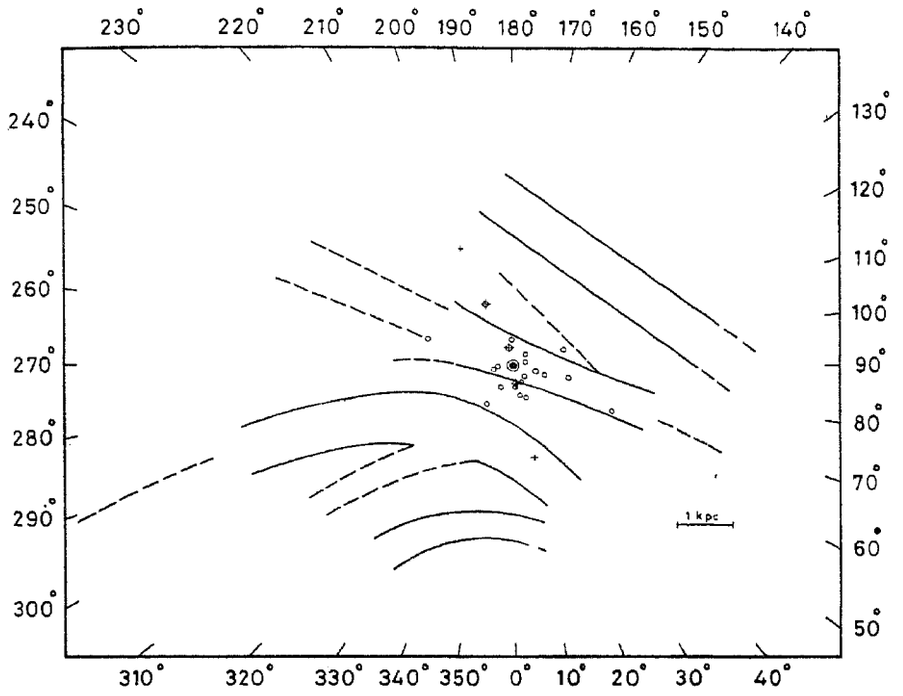

Figure 10. The galactic distribution of Cepheids for which spectroscopic abundances are available. Spiral arms are traced from Humphreys (1978). Sun's position is shown by ⊙ symbol. Programme Cepheids are shown by + symbol.

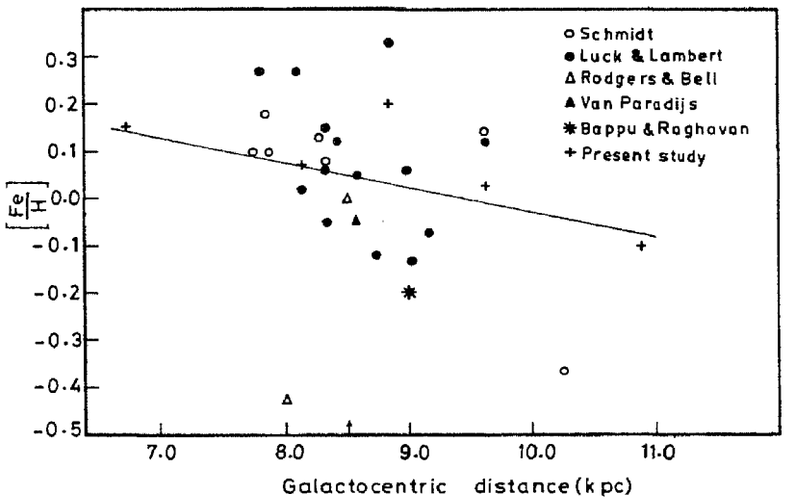

Figure 11. The galactic radial abundance gradient in Fe/H. Sun's galactocentric position is shown by an arrow.

Washington photometric system, determined photometric abundances of a large number of Cepheids covering a wide range of galactocentric distances (5 to 15 kpc). He derived an abundance gradient

$(d[A/H])/dr_{gc} = -0.07.$

Janes (1979) obtained a gradient of − 0.05 from the DDO photometry of a large number of K giants. Using the iron abundances derived from the earlier studies of supergiants and Cepheids (LL ; Luck & Bond 1980), Luck (1982) derived a radial abundance gradient

$$(d[\mathrm{Fe/H}])/dr_{gc} = -0.13 \pm 0.03$$

which is steeper than any abundance gradient determined so far. Pagel & Edmunds (1981) have questioned the use of supergiants for a determination of the radial abundance gradient, since the atmospheric abundances of these stars could be modified due to mixing with the interiors. The present investigation covers a larger range of galactocentric distances (6.7 − 10.8 kpc) than that of Luck (7.7 − 10.6 kpc). Using the iron abundances and excluding ζ Gem which is known to be metal rich for its position in galactic disk, we derive the relation

$$[\mathrm{Fe/H}] = -0.056\, r_{gc} + 0.53$$
$$\pm 0.008 \quad \pm 0.007$$

with a correlation coefficient of ∓ 0.97. This gradient is in close agreement with the ones derived by Janes (1979) and Harris (1981). This value also agrees with the one derived from the total sample of 30 points, inclusive of Luck's sample. Relatively smaller range in galactocentric distances covered by Luck (~ 30 per cent smaller than our range) and inaccuracies in the distance estimates for supergiants may be partly responsible for this discrepancy. The metal-richness of ζ Gem for its position in the solar neighbourhood can be explained in terms of its birthsite with respect to the density wave (Giridhar 1983).

5.3 *Variation of* [*s*/Fe] *across the Disk*

The iron-peak nuclei are formed by explosive nucleosynthesis within supernovae whereas *s*-process elements are formed by slow neutron capture by heavy elements in the interiors of red giants. These two processes occur in different ranges of mass (2-4 $M_\odot$ for red giants and 8-15 $M_\odot$ for supernovae with the present uncertainty about whether 4-8 $M_\odot$ stars end as planetary nebulae or supernovae). Thus the abundance ratio [*s*/Fe] at different times in the history of the galaxy and the variation of [*s*/Fe] across the galactic disk may provide important constraints on the theories of galactic evolution.

For metal-deficient stars of the halo population, Spite & Spite (1978) found the *s*-process element barium and − to a certain extent − yttrium to be overdeficient. This over-deficiency decreases when [Fe/H] increases and becomes negligible for [Fe/H] > − 1.5.

From an analysis of a homogeneous group of old metal-poor F and G stars in the galactic disk, Huggins & Williams (1974) found a correlation between [*s*/Fe] and [Fe/H]. They interpreted this correlation as evidence that heavier *s*-process metals of the interstellar medium in the disk have increased more rapidly than the overall metal abundance, during the time interval covered by the formation of these stars.

In the present investigation, we have determined the abundances of *s*-process elements Ba, La, Ce and Sm. These elements present themselves in very few lines in the

stellar spectra. This fact increases the uncertainty of the abundance estimates. The use of a composite *s*-process index

$$S = 1/N \sum_{i=1}^{N} [s/\mathrm{Fe}]$$

has been suggested by Huggins & Williams (1974). These composite indices have the advantage of reduced scatter, though the information about individual elements is lost. In Table 8 we give [Fe/H], [Ba/Fe], [La/Fe], [Ce/Fe] and [Sm/Fe] for our programme stars and the composite indices

$$S_1 = \tfrac{1}{4}([\mathrm{Ba/Fe}] + [\mathrm{Ce/Fe}] + [\mathrm{La/Fe}] + [\mathrm{Sm/Fe}])$$

and

$$S_2 = \tfrac{1}{3}([\mathrm{Ba/Fe}] + [\mathrm{Ce/Fe}] + [\mathrm{Sm/Fe}]).$$

For two of our stars, La abundances were not determined, so only S_2 could be determined.

We have plotted in Fig. 12 [*s*/Fe] and S_2 as a function of galactocentric distance. A straight line fit to S_2 and r_{gc} data yields

$$\begin{array}{lll} S_2 = & 0.018012\ [r_{gc}] & -0.251 \quad (n=5) \\ & \pm 0.02039 & \pm 0.182 \end{array}$$

with a correlation coefficient $r = 0.367$. Thus, there is no significant trend between S_2 and the galactocentric distance, implying that the rate of enrichment of *s*-process elements is essentially the same as that of [Fe/H]. We have plotted [*s*/Fe] as a function of [Fe/H] in Fig. 13. A straight-line fit so S_2 and [Fe/H] data yields

$$\begin{array}{lll} S_2 = & -0.008\ [\mathrm{Fe/H}] & -0.091 \quad (n=5) \\ & \pm 0.294 & \pm 0.037 \end{array}$$

with a correlation coefficient $r = -0.013$. Thus S_2 and [Fe/H] are not correlated.

In the simple model of galactic evolution based on the assumption of evolution in isolated well-mixed zones with no initial enrichment, the abundance of *s*-process elements is predicted to vary as $[\mathrm{Fe/H}]^2$. With the inclusion of prompt initial enrichment (PIE) to account for the observed narrow range of metallicity distribution of G dwarf stars, the abundance of *s*-process elements are no longer expected to vary so fast; still, the predicted abundance variation for *s*-process elements is faster than that for [Fe/H]. In other words, there should be a positive correlation between [*s*/Fe] and [Fe/H]. The correlation obtained by Spite & Spite (1978) and Huggins & Williams (1974) may favour the enrichment predicted by a simple model, but the absence of any significant

Table 8. Abundance of *s*-process elements in the Cepheids.

Star	r_{gc}	[Fe/H]	[Ba/Fe]	[La/Fe]	[Ce/Fe]	[Sm/Fe]	S_1	S_2
WZ Sgr	6.73	+0.15	0.0	−0.10	−0.25	−0.05	−0.10	−0.10
X Sgr	8.13	+0.07	−0.09		−0.27	−0.27		−0.21
ζ Gem	8.83	+0.20	−0.15		−0.05	+0.03		−0.06
T Mon	9.61	+0.03	+0.07	−0.13	+0.03	−0.12	−0.04	−0.005
SV Mon	10.87	−0.10	0.0	−0.10	−0.17	−0.10	−0.09	−0.09

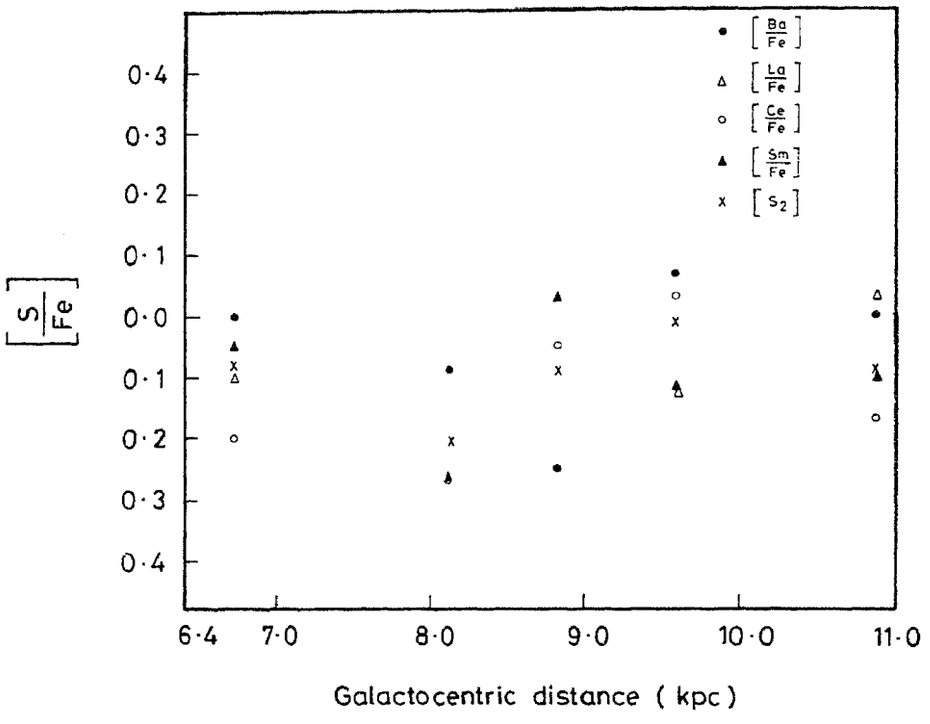

Figure 12. A plot of [*s*/Fe] as a function of galactocentric distance.

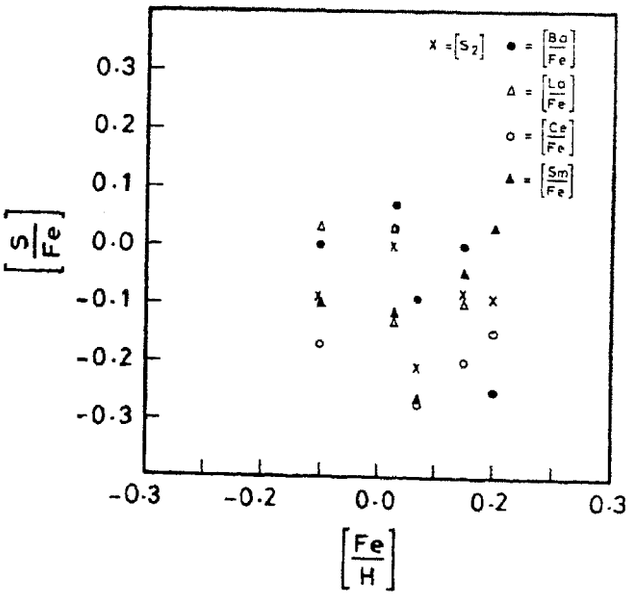

Figure 13. A plot of [*s*/Fe] against [Fe/H].

correlation for young disk stars cannot be explained by a simple model.

Instead of a closed system, a model with steady infall of unprocessed material has been developed by Larson (1974, 1976). In the infall models, the observed metallicity distribution can be explained without requiring an initial burst of massive stars (PIE). The infalling metal poor gas produces a dilution effect which counteracts the enrichment of ISM and hence an asymptotic variation of [*s*/H] and [Fe/H] are predicted. Thus the ratio does not change after [*s*/Fe], [*s*/H] and [Fe/H] reach their asymptotic values. The lack of correlation between [*s*/Fe] and [Fe/H] for the young disk stars found in the present investigation favours an infall model of galactic evolution.

An alternative explanation can be based on the hypothesis of a variable initial mass function (IMF). Whereas Fe is produced in explosive nucleosynthesis in supernova explosions of massive stars, *s*-process elements are synthesized in the intermediate-mass stars. Thus [*s*/Fe] at a given time is related to the ratio of intermediate- to high-mass stars. A comparison of [*s*/Fe] in old and young stars may provide useful information on the variation of IMF in the course of galactic evolution. In a simple intuitive way, we can say that the fast enrichment of *s*-process nuclei in the old halo population stars is due to a steeper IMF at the time of formation of spheroidal population. After the formation of the disk, the IMF may have become flatter due to an increased metallicity and resultant efficiency in cooling of clouds. Hence the abundance of *s*-process elements for the disk does not show the steady enrichment as exhibited by halo stars. It should be borne in mind that the assumption of a constant IMF has been made in the models of chemical evolution of galaxies only out of ignorance on star formation processes. The density wave can compress the cold gas clouds in the young disk and form massive stars. Such conditions may not exist in the absence of a density wave.

Clegg, Lambert & Tomkin (1981) have recommended the use of oxygen rather than iron as the primary elements relevant to *s*-process nuclei in the disc. More accurate abundance estimates are required – both for oxygen and the *s*-process elements – to verify such a correlation.

5.4 *Summary of Conclusions*

The major conclusions that have been drawn from the present study of the abundances in Cepheid atmospheres are the following:

(1) There is gradient in [Fe/H] in the disk between the galactocentric distances 6.74 – 10.87 kpc. The value of the gradient -0.056 ± 0.008 derived by us agrees with the general sample of Cepheids for which spectroscopic abundances are available, and also with the photometric gradients -0.07 and -0.05 derived by Harris (1981) and Janes (1979) respectively.

(2) The *s*-process enrichment of the young galactic disk takes place at the same rate as the Fe enrichment, indicating that the high-mass stars are possibly formed at a higher rate in the young disk than in the halo, and probably, in the old disk.

6. Discussion and future prospects

In the present investigation, we have demonstrated a successful application of the method of spectrum synthesis in dealing with the problems of blending of spectral lines which has been a major handicap in conventional abundance determinations. For spectral types later than G0, the crowding of lines becomes increasingly severe. This

problem cannot be solved only by increasing the resolution. In a given spectral region, if the frequency of lines is larger than the reciprocal of the line width, all the spectral lines of the region will be intrinsically blended and increasing the resolution will not separate these lines. Also, in the case of elements like *s*-process elements which present themselves in a very few and often blended features, the abundance determination at a dispersion of 22.6 Å mm^{-1} employed in the present investigation would have been an impossible task without the spectrum synthesis technique.

Our review of the existing spectroscopic abundances for Cepheids shows that spectroscopic abundances are known only for 21 Cepheids. The Cepheids studied spectroscopically prior to this investigation are brighter than visual magnitude 7.0, since higher dispersions were considered necessary. We have demonstrated that the synthesis method is applicable even at somewhat lower dispersion, thus enabling one to reach fainter and farther. The total number of Cepheids with $m_v \lesssim 8.5$ is around 90; all these stars are well within the reach of a medium-size telescope.

In order to study the chemical evolution of the halo, metal-deficent high-velocity stars are currently used. An abundance gradient perpendicular to the plane of the Galaxy was discovered by Trefzger (1981). W Virginis stars which belong to the halo population also follow their own period-luminosity relation. One can obtain a more accurate distribution of chemical composition perpendicular to the galactic plane by utilizing these stars for which accurate distances can be determined.

Accurate abundance determinations require good models for line-forming regions, *i.e.*, model atmospheres. A number of semi-empirical relations based on the limb-darkening data have been constructed for the Sun. But for other stars only theoretical models are available. A straight-forward way of checking the adequacy of model atmospheres is by comparing the fluxes predicted by them at different wavelengths with the observed fluxes. Detailed comparisons for G-K stars show good agreement in general but there is a discrepancy in the ultraviolet region; the fluxes predicted by theoretical models are higher than the observed ones. This difference becomes larger for red gaints. In the case of gaints the difference is proportional to the logarithmic metal abundance, and is negligible for population II stars (Gustafsson & Bell 1979). It is believed that the discrepancy arises due to an unconsidered opacity source which is sensitive to metallicity. Holweger (1970) had already suggested that a haze of weak spectral lines not included in the extensive line list used in the model atmosphere calculation, could be a source of extra opacity. The effect on the temperature structure of this extra opacity as estimated by Gustafsson *et al.* (1975) is $\sim$ 100 K. An attempt to study these weak lines in laboratory spectra of iron should be undertaken.

We have used the solar gf values for the lines used in the present investigation. These values are derived using solar equivalent widths and a good model solar atmosphere. However, in the list of wavelengths of solar lines (Moore, Minnaert & Houtgast 1966), some lines remain unidentified. We omitted in our work the spectral regions with such unknown lines. Thus we had to leave out some of the important lines of *s*-process elements due to the presence of unidentified lines in their close neighbourhood. Detailed laboratory investigations of a number of elements are required for the identification of such lines.

We have indicated a few steps which would lead to the determintion of accurate

abundances. The importance of accurate abundance determination need hardly be exaggerated. A radical change in the understanding of nucleosynthesis in stars and of chemical evolution of the Galaxy may appear when very accurate abundance estimates for stars of different age groups are available as a function of their galactocentric position.

Acknowledgements

This paper incorporates the material presented as doctoral thesis to the Ravishankar University, Raipur. I am indebted to late Professor M. K. Vainu Bappu for suggesting the topic, for guidance and encouragement, for the generous allotment of observing time with the telescope and computing time with the TDC-316 computer of the Indian Institute of Astrophysics. I am also thankful to Professor J. C. Bhattacharyya for helping me to complete this work after the demise of Professor Bappu. I thank Dr N. Kameswara Rao for giving me Sneden's code and for many useful discussions. I acknowledge the help of A. V. Ananth and other staff of the computer section, of T. P. Prabhu and P. Venkatakrishnan, and of several friends and colleagues at the Institute without which this work would have been more difficult to accomplish. I am also thankful to an anonymous referee for valuable comments which enabled me to improve the paper considerably.

References

Abt, A. 1952, *Astrophys. J.*, **115,** 199.

Allen, C. W. 1973, *Astrophysical Quantities*, 3 edn, University of London, Athlone Press.

Bappu, M. K. V., Raghavan, N. 1969, *Mon. Not. R. astr. Soc.*, **142,** 295.

Becker, W., Fenkart, R. 1970, in *IAU Symp 38: The Spiral Structure of our Galaxy*, Eds W. Becker and G. Contopoulos, D. Reidel, Dordrecht, p. 205.

Bell, R. A., Eriksson, K., Gustafsson, B., Nordlund, A. 1976, *Astr. Astrophys. Suppl. Ser.*, **23,** 37.

Benvenuti, P., D'Odorico, S., Peimbert, M. 1973, *Astr. Astrophys.*, **28,** 447.

Blackwell, D. E., Shallis M. J. 1979, *Mon. Not. R. astr. Soc.*, **186,** 669.

Clegg, R. E. S., Lambert, D. L., Tomkin, J. 1981, *Astrophys. J.*, **250,** 262.

Comte, G. 1975, *Astr. Astrophys.*, **39,** 197.

Cowley, C. R. 1970, *The Theory of Stellar Spectra*, Gordon and Breach, New York.

de Vaucouleurs, G. 1968, *Appl. Opt.*, **7,** 1513.

Eggen, O. J. 1951, *Astrophys. J.*, **113,** 367.

Eggen, O. J. 1969, *Astrophys. J.*, **156,** 617.

Evans, T. L. 1968, *Mon. Not. R. astr. Soc.*, **141,** 109.

Foy, R. 1972, *Astr. Astrophys.*, **18,** 26.

Giridhar, S. 1982, *PhD thesis*, Ravishankar University, Raipur.

Giridhar, S. 1983, in preparation.

Grenon, M. 1972, in *IAU Coll. 17: L'age des Etoiles*, Eds G. Cayrel de Strobel and A. M. Delplace, Meudon Observatory, Paris, Chapter 55.

Gustafsson, B., Bell, R. A., Eriksson, K., Nordlund, A. 1975, *Astr. Astrophys.*, **42,** 407.

Gustafsson, B., Bell, R. A. 1979, *Astr. Astrophys.*, **74,** 313.

Harris, H. C. 1981, *Astr. J.*, **86,** 707.

Hawley, S. A. 1977, *Bull. am. astr. Soc.*, **9,** 374.

Holweger, H. 1970, *Astr. Astrophys.*, **4,** 11.

Holweger, H., Müller, E. A. 1974, *Solar Phys.*, **39,** 19.

Huggins, P. J., Williams, P. M. 1974, *Mon. Not. R. astr. Soc.*, **169,** 1P.

Humphreys, R. M. 1978, in *IAU Symp. 84: The Large Scale Characteristics of the Galaxy,* Ed. W. B. Burton, D. Reidel, Dordrecht, p. 93.

Janes K. A. 1977, in *IAU Coll. 45: Chemical and Dynamical Evolution of our Galaxy,* Eds E. Basinska GrZesik and M. Mayor, Geneva Observatory, p. 173.

Janes, K. A. 1979, *Astrophys. J. Suppl. Ser.*, **39,** 135.

Janes, K. A., McClure, R. D. 1972, in *IAU Coll. 17: L'age des etoiles,* Eds G. Cayrel de Strobel and A. M. Delplace, Meudon Observatory, Paris, Chapter 28.

Joy, A. A. 1937, *Astrophys. J.*, **86,** 363.

Keller, C. F., Murschlecner, J. P. 1970, *Astrophys. J.*,**161,** 217.

Kraft, R. P. 1967, in *IAU Symp. 28: Aerodynamic Phenomena in Stellar Atmospheres,* Ed. R. N. Thomas, Academic Press, New York, p. 207.

Kukarkin, B. V., Kholopov, P. N., Efremov, Yu. N. Kurkina, N., Kurochkin, N. E., Medvedeva, G. I., Perova, N. N., Fedorovich, V. P., Frovlov, M. S. 1969, *General Catalogue of Variable Stars,* Astronomical Council of the Academy of Sciences, Moscow.

Kurucz, R. L. 1975, in *Multicolour Photometry and HR Diagram,* Eds A. G. Davis Philip and D. S. Hayes, Dudley Obs. Rep. No. 9, 271.

Kurucz, R. L. 1979, *Astrophys. J. Suppl. Ser.*, **40,** 1.

Kurucz, R. L., Peytremann, E. 1975, *Smithsonian Astrophys. Obs. Spec. Rep.*, No. 362.

Larson, R. B. 1974, *Mon. Not. R. astr. Soc.*, **166,** 585.

Larson, R. B. 1976, *Mon. Not. R. astr. Soc.*, **176,** 31.

Lites, B. W., Cowley, C. R. 1974, *Astr. Astrophys.*, **31,** 361.

Luck, R. E. 1982, *Astrophys. J.*, **256,** 177.

Luck, R. E., Bond, H. E. 1980, *Astrophys. J.*, **241**, 214.

Luck, R. E., Lambert, D. L. 1981, *Astrophys. J.*, **245,** 1018 (LL).

Mariska, J. T., Doschek, G. A., Feldman, U. 1980, *Astrophys. J.*, **242,** 1083.

May, M., Richler, J., Wichelmann, J. 1974, *Astr. Astrophys. Suppl Ser.*, **18,** 405.

Mayor, M. 1976, *Astr. Astrophys.*, **48,** 301.

Mitchell, R., Iriarte, B., Steinmetz, D., Johnson, H. L. 1964, *Bol. Obs. Tonantzintla Tacubaya,* **3,** 153.

Moore, C. E. 1945, *Contr. Princeton University,* No. 20, 1.

Moore, C. E., Minnaert, M. G. J., Houtgast, J. 1966, *The Solar Spectrum 2935A to 8770 A,* N. B. S. Monograph.

Nikolov, N. C., Ivanov, G. R. 1974, *Variable Stars,* **20,** 63.

Pagel, B. E. J. 1977, in *Proc. Second Symp. on Origin and Distribution of the Elements,* UNESCO, Paris. p. 79.

Pagel, B. E. J., Edmunds, M. G. 1981, *A. Rev. Astr. Astrophys.*, **19,** 77.

Parsons, S. B. 1969, *Astrophys. J. Suppl. Ser.*, **18,** 127.

Parsons, S. B. 1971, *Mon. Not. R. astr. Soc.*, **152,** 121.

Peimbert, M. 1979, in *IAU Symp. 84: The Large Scale Characteristics of the Galaxy,* Ed. W. B. Burton, D. Reidel, Dordrecht, p. 79.

Peimbert, M., Serrano, A. 1980, *Rev. Mex. Astr. Astrofis.*, **5,** 9.

Peimbert, M., Torres-Peimbert, S., Rayo, J. F. 1978, *Astrophys. J.*, **220,** 516.

Pel, J. W. 1976, *Astr. Astrophys. Suppl. Ser.*, **24,** 413.

Pel, J. W. 1978, *Astr. Astrophys.* **62,** 75.

Rautela, B. S., Joshi, S. C. 1976, *Astrophys. Space Sci.*, **40,** 455.

Rodgers, A. W., Bell, R. A. 1968, *Mon. Not. R. astr. Soc.*, **138,** 23.

Rutten, R. 1976, *Solar Eclipse Observations and Ban Line Formation,* Utrecht Observatory.

Sandage, A., Tammann, G. A. 1968, *Astrophys. J.*, **151,** 531.

Sandage, A., Tammann, G. A. 1969, *Astrophys. J.*, **157,** 683.

Schaltenbrand, R., Tammann, G. A. 1971, *Astr. Astrophys. Suppl. Ser.*, **4,** 265.

Schmidt, E. G. 1971, *Astrophys. J.*, **170,** 109.

Schmidt, E. G. 1972, *Astrophys. J.*, **174,** 605.

Schmidt, E. G., Rosendhal, J. D., Jewsbury. C. P. 1974, *Astrophys. J.*, **189,** 293.

Searle, L. 1971, *Astrophys. J.*, **168,** 327.

Sneden, C. A. 1974, *PhD Thesis,* University of Texas, Austin.

Spite, M., Spite, F. 1978, *Astr. Astrophys.* **67,** 23.

Stibbs, D. W. N. 1955, *Mon. Not. R. astr. Soc.*, **115,** 363.

Tammann, G. A. 1970, in *IAU Symp. 38: The Spiral Structure of our Galaxy,* Eds W. Becker and G. Contopoulos, D. Reidel, Dordrecht, p. 236.

Torres-Peimbert, S., Peimbert, M. 1977, *Rev. Mex. Astr. Astrofis.*, **2,** 181.

Trefzger, C. G. 1981, *Astr. Astrophys.*, **95,** 184.

Tsarevsky, G. S. 1967, *Inf. Bull. Var. Stars.*, No. 176.

Unsöld, A. 1955, *Physik der Sternatmosphären,* 2 edn, Springer-Verlag, Berlin.

Van Paradijs, J. A. 1971, *Astr. Astrophys.*, **11,** 229.

Viswanath, C. 1981, *Kodaikanal Obs. Bull. Ser. A.*, **3,** 57.

Walraven, J. H., Tinbergen, J., Walraven, T. H. 1964, *Bull. astr. Inst. Netherl.*, **17,** 520.

Whaling, W., Scalo, J. M. Testerman L. 1977, *Astrophys. J.*, **212,** 581.

Wolff, S. C., Wallerstein, G. 1966, *Astrophys. J.*, **144,** 419.

Wolnik, S. J., Berthel, R. O. 1973, *Astrophys. J.*, **179,** 665.

Wisniewski, W. Z., Johnson, H. L. 1968, *Commu. Lunar Planet. Lab.*, **7,** 57.